ARES

Accelerating cavity Resonantly coupled with an Energy Storage

T. Kageyama, K. Akai, N. Akasaka, E. Ezura, F. Naito, T. Shintake, Y. Takeuchi, and Y. Yamazaki

The ARES scheme is that an accelerating cavity is coupled with an energy storage cavity via a coupling cavity.

A large energy storage cavity operated in a high-Q mode (TE01n) is employed to reduce the detuning frequency of the cavity under heavy beam loading.

It is needless to say that the accelerating cavity itself must be a HOM-damped structure.

This scheme is expected to be a breakthrough in development of the normal conducting cavity for KEKB.

1) ARES Cavity System
   a) Basic RF Design
   b) Numerical Analysis using MAFIA
   c) Results of Cold Model Tests

2) HOM-damped Cavity employed in the ARES scheme
   a) RF Design
   b) Development of a High-Power Test Cavity
   c) Microwave Absorber
   d) Results of High-Power Test

A scheme of employing an energy storage cavity operated in a low-loss mode (TE015) was first pointed out by Shintake to increase the stored energy while the total power dissipation is kept below a reasonable level.

A couple of problems should be solved to realize this scheme.

1) The instability will arise from a parasitic mode (0 mode) existing near the accelerating mode (π mode). The coupling impedance of the parasitic mode has the same order of magnitude as that of the accelerating mode.

2) The field amplitude and phase of the π mode is unstable against heavy beam loading.

In order to solve these problems, Yamazaki has proposed introducing a coupling cavity between the accelerating and storage cavities and employing the $\pi/2$ mode as the operating mode.

This three-cavity system ARES has the following advantages over the former two-cavity system where an accelerating cavity is directly coupled with a storage cavity.

1) The operating mode of the ARES cavity is the $\pi/2$ mode, which has excellent field stability against heavy beam loading.

2) The stored energy ratio Us/Ua can be adjusted by changing the coupling factor ratio ka/ks.

3) The $\pi/2$ mode has almost no field excited in the coupling cavity. Therefore, the two parasitic modes (the 0 and π modes) can be selectively damped by installing a coupler in the coupling cavity, while the $\pi/2$ mode is not affected.

4) The 0 and π modes are located nearly symmetrically with respect to the $\pi/2$ mode. Therefore, the contributions of the impedances of the damped parasitic modes to the instability are expected to be counterbalanced each other.

Storage Cavity Design

A Cylindrical Cavity
operated in the TE015 mode (f = 509 MHz)

diameter = 1100 mm
axial length = 2000 mm
Q = 260000

The storage cavity has many parasitic modes near the TE015 mode. Therefore, careful tuning of the cavity dimensions is required to prevent the parasitic mode mixing to the TE015 mode.

1) The circumference of each end-plate is grooved to resolve the degeneracy of the TE015 and TM115 modes.

2) To minimize the effect of the coupling slot on the parasitic mode mixing, the TEmnp(p=odd) and TMmnp(m>0, p=odd) modes must be kept away from the TE015 mode.

Basic RF Design of the ARES Cavity

The first design started with the most simple case: a cylindrical accelerating cavity is coupled with the storage cavity via a cylindrical coupling cavity.

Design Criteria

1) Each cavity should be tuned to the operating frequency of 508 MHz under the $\pi/2$-mode boundary condition.

2) The stored energy in the storage cavity should be larger than that in the accelerating cavity by factor 10.

$Us/Ua > 10$

3) The 0 and π modes should be nearly symmetrically located with respect to the $\pi/2$ mode.

Summary of the Numerical Analysis

1) The R/Q value of the ARES cavity can be reduced by an order of magnitude compared to that of a conventional single-cell copper cavity.

2) The Q value of the ARES cavity is about five times as large as that of a conventional copper cavity.

3) The shunt impedance of the ARES cavity is kept at a reasonable level.

4) The growth time of the instability due to the accelerating mode is longer than 30 ms in LER.

5) Installing a coupler in the coupling cavity will make the growth time of the instability due to the parasitic modes longer than 10 ms.

Cold Model Tests

Two aluminum 1/5 scale models were fabricated to confirm the numerical analysis.

The coupling cavity of the first model is a simple pillbox cavity.

The coupling cavity of the second model has two coupler ports for damping the parasitic modes.

Summary of Cold Model Tests

1) The measured Q value of the $\pi/2$ mode was 33000, which corresponds to 140000 (85% of the calculated value) for a full scale copper ARES cavity.

2) The bead perturbation measurement showed that the R/Q value was reduced by a factor of 0.069, which is in good agreement with the calculated value of 0.065.

3) The 0 and π modes were damped enough by the couplers installed in the coupling cavity. The growth time of the instability due to both modes is calculated to be 17 ms for LER.

Development of the HOM-damped accelerating cavity

HOM damped scheme:
The cavity is loaded with a large coaxial waveguide equipped with a notch filter. The filter blocks the TEM wave coupled with the accelerating mode while passing other waves coupled with the cavity HOMs.
(Damped structures with this scheme were devised by Shintake and by Akai, independently of each other.)

HOM waves are absorbed by bullet-shape sintered SiC ceramics.

A high-power test model has been designed and built to demonstrate the performance in high power operation and the fabrication technologies involved.

The test cavity has been successfully operated up to 110 kW RF input power (the design value = 75 kW).

RF Design

The gap dimensions of the filter and coaxial waveguide were carefully determined to avoid multipactoring discharge at the operating frequency.

The beam bore diameter was increased to 145 mm in order to lower the TM01 and TE11 cutoff frequencies below the second stop frequency of the notch filter.

The filter position along the waveguide, represented by the distance *l*, affects not only the shunt impedance of the accelerating mode, but also the HOM damping properties.

The distance *l* was determined to be 120 mm, which gives better HOM damping.

HOM Absorber

For HOM absorption, 16 bullet-shape sintered SiC ceramics (dia. = 40 mm and length = 400 mm) are employed per cavity.

Structural, Thermal, and Vacuum Properties of SiC

fine and dense ceramics	
high mechanical strength	
good thermal conductivity	120 W/mK
	(230 W/mk Aluminum)
low outgassing rate	

In KEK 2.5-GeV electron linac, about 200 SiC absorbers (dia.=24mm, length=300mm) have been used for the S-band waveguide loads without any trouble for 10 years.

High-Power Test of SiC Absorber

High-power test of a prototype SiC absorber was carried out using a pulsed klystron (f = 1296 MHz).

A metal O ring was used for vacuum seal between the SiC ceramics and the SUS flange.

The SiC absorber functioned normally up to an average RF power of 2.8 kW (a peak power of 105 kW with a pulse width of 540 μs at 50 Hz) without any vacuum, thermal, or discharge trouble.

For vacuum seal for SiC, we are also planning to braze a thin copper sleeve to the SiC ceramics.

High-power test of the prototype HOM-damped cavity

Setup

A TRISTAN APS input coupler (capable of 300 kW transmission power) was used for RF power feed. This coupler uses a loop coupling and has a cylindrical ceramic window at the rectangular-to-coaxial transition.

A TRISTAN APS tuner was used for tuning the cavity in high power operation. The tuner has a 7-cm-diameter plunger with about 6 cm of travel, which gives a tuning range of about 1.8 MHz.

The whole cavity system was cooled by 100 l/min of water: 70 l/min for the cavity cooling circuits, 10 l/min for the input coupler and the tuner, and 20 l/min for the SiC absorbers.

RF conditioning

RF power was supplied by a CW klystron (Toshiba E3786).

RF conditioning was continuously carried out keeping the vacuum pressure below 5×10^{-7} Torr.

It took about four hours to go above 0.5 kW. That was probably due to multipactoring discharge in the coaxial waveguide or in the notch filter.

The test cavity was conditioned up to 90 kW in about 33 hours and then the first RF conditioning was ended. Finally, the cavity was tested up to 110 kW.

Small gas bursts were frequently observed above 80 kW, and similar events were sometimes observed at 40 kW. Further RF conditioning is planned for more stable high-power operation.

Summary

Numerical simulation studies and cold model measurements showed that the ARES scheme works as expected.

We have demonstrated the high-power performance of the HOM-damped accelerating structure and that of the SiC microwave absorber.

However, further R&D work is required for more stable high-power operation and for an ARES scheme employing this damped structure.

The first high-power ARES cavity will be built by March 1996. Its beam test is also scheduled in the fall of 1996.

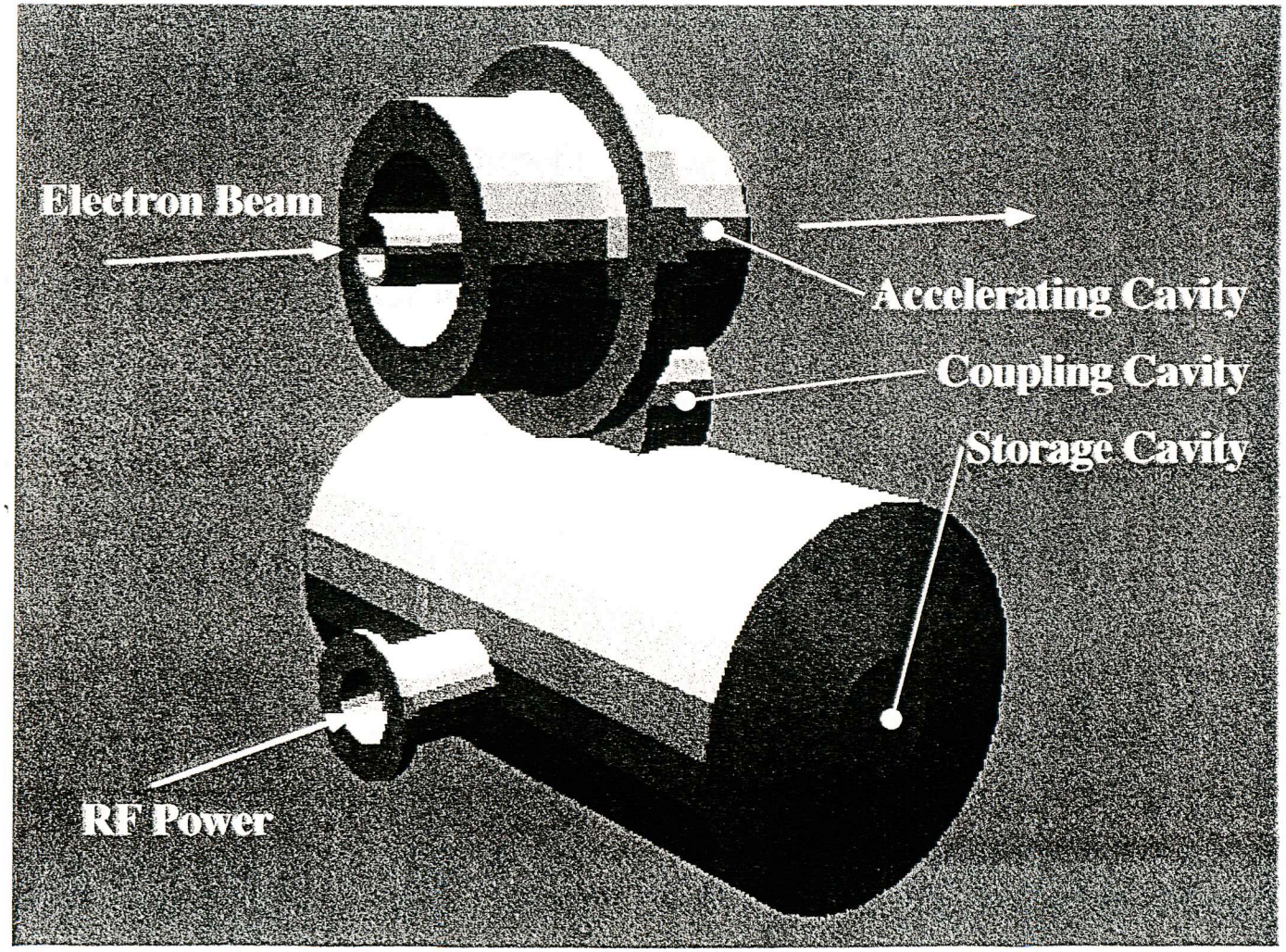

Accelerator Resonantly coupled with Energy Storage (ARES)
for KEKB

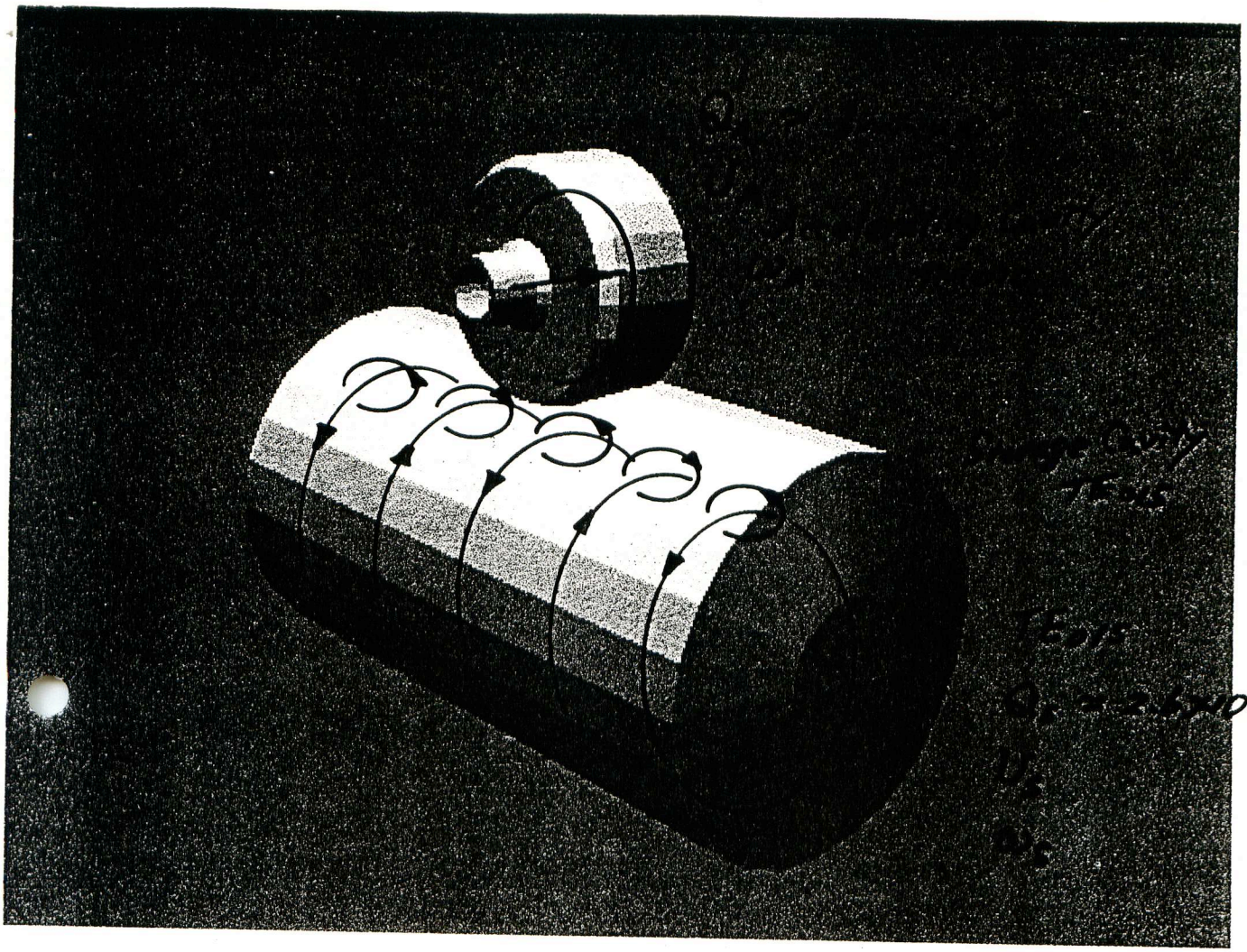

π mode

← E field

← H field

$$\left(\frac{R}{Q}\right)_{ARES} = \frac{\left(\frac{R}{Q}\right)_A}{1 + U_S/U_A}$$

for the π mode $\quad U_S/U_A = 1$

($U_S/U_A \gg 1$ means $\omega_A \neq \omega_S$!)

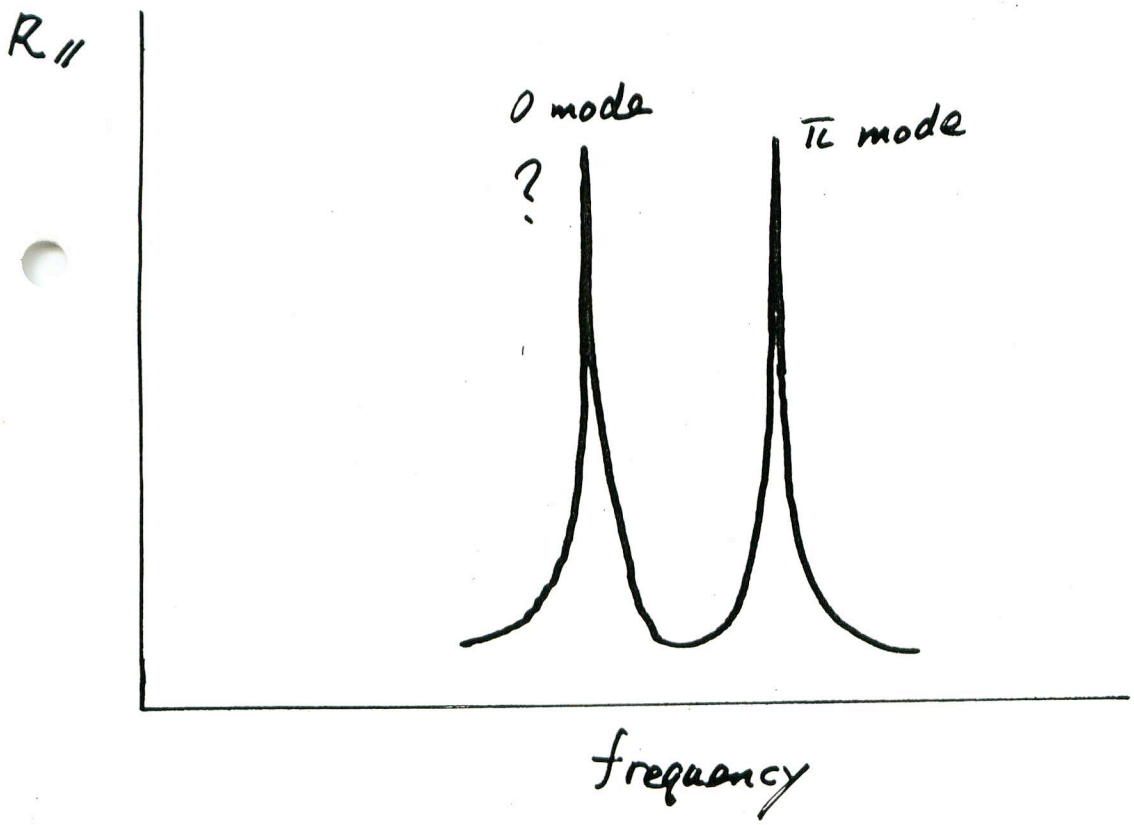
$R_{//}$
0 mode
?
π mode
frequency

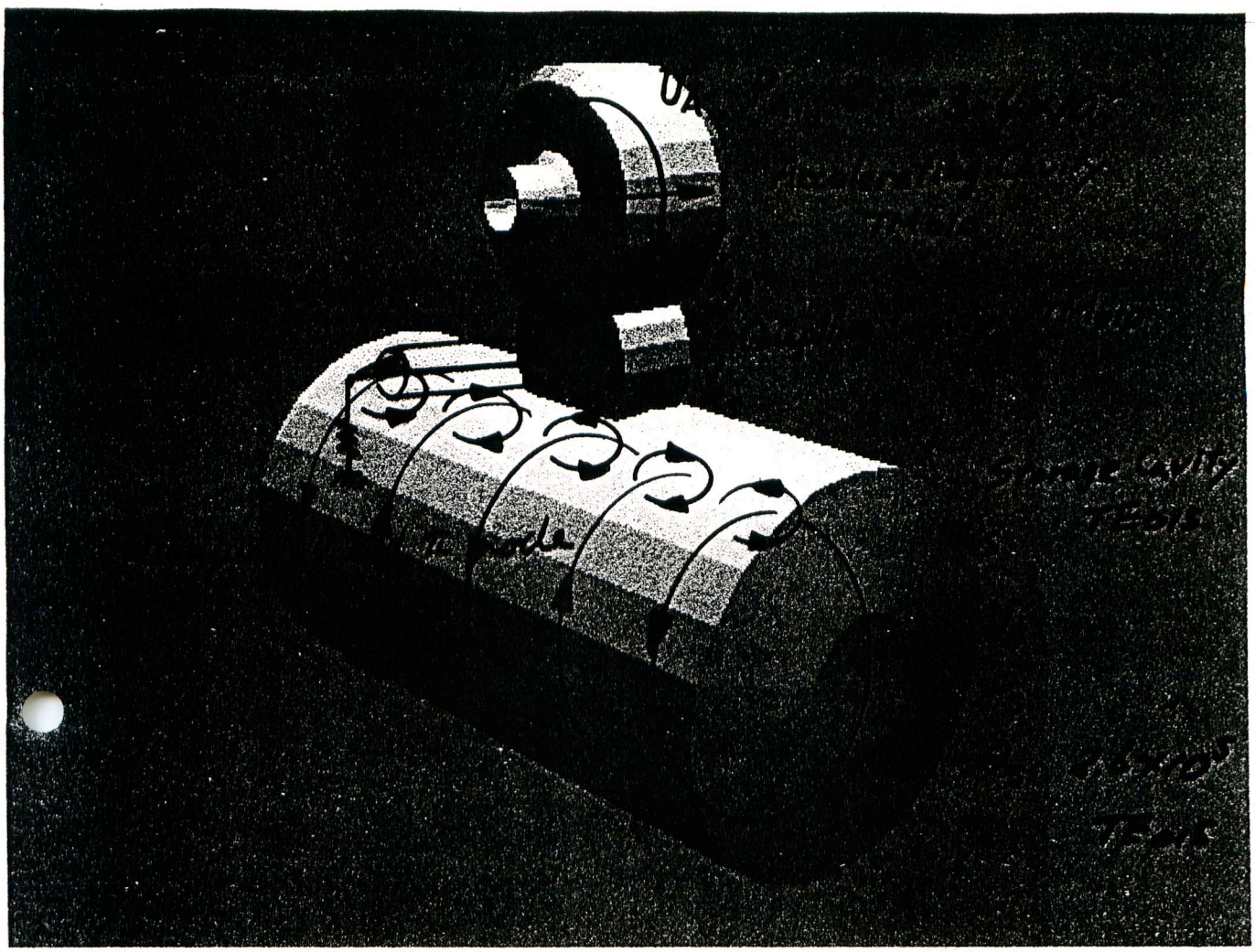

$\pi/2$ Accelerating Mode

← E field

← H field

$$\left(\frac{R}{Q}\right)_{ARES} = \frac{\left(\frac{R}{Q}\right)_A}{1 + U_S/U_A}$$

$$Q_{ARES} = \frac{\omega_0 U_A + \omega_0 U_S}{P_A + P_S}$$

$$R_{ARES} = \frac{R_A}{1 + P_S/P_A} = \frac{R_A}{1 + \frac{Q_A}{Q_S}\cdot\frac{U_S}{U_A}} \simeq \frac{R_A}{3}$$

$$\frac{U_S}{U_A} \simeq 10 \qquad \frac{Q_A}{Q_S} \simeq \frac{1}{5}$$

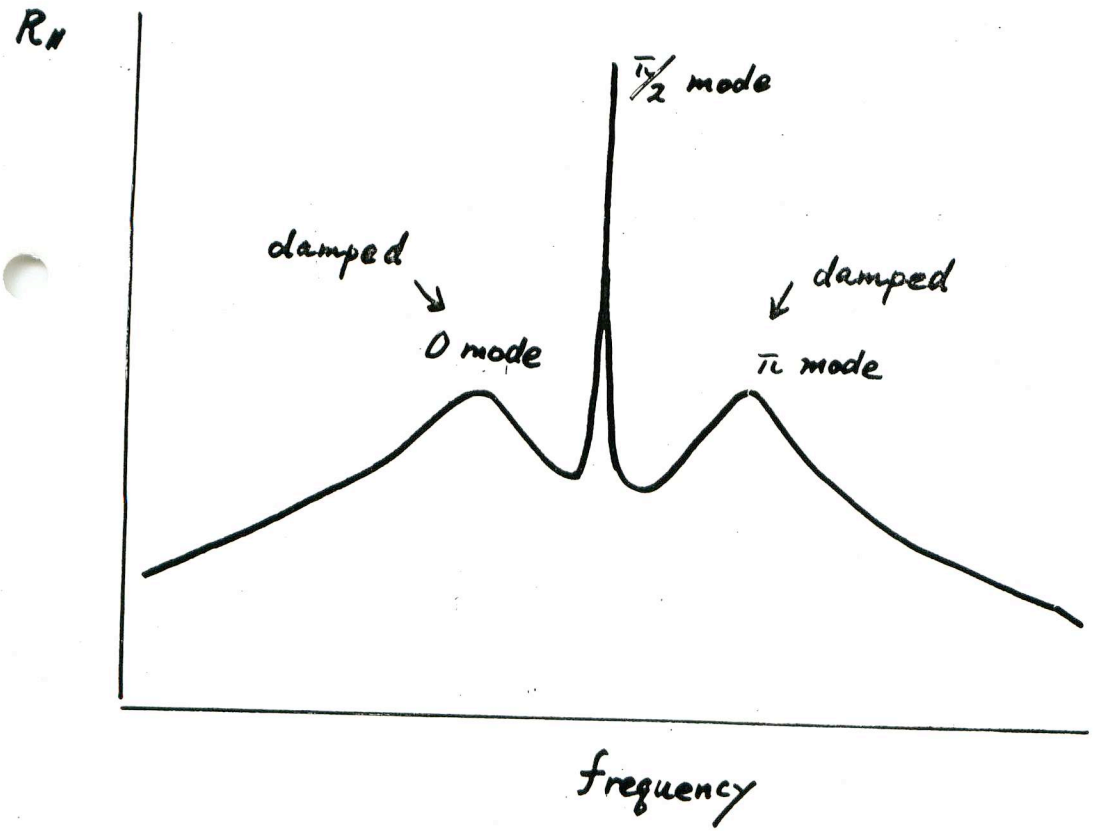
R_{II}
$\pi/2$ mode
damped
0 mode
damped
π mode
frequency

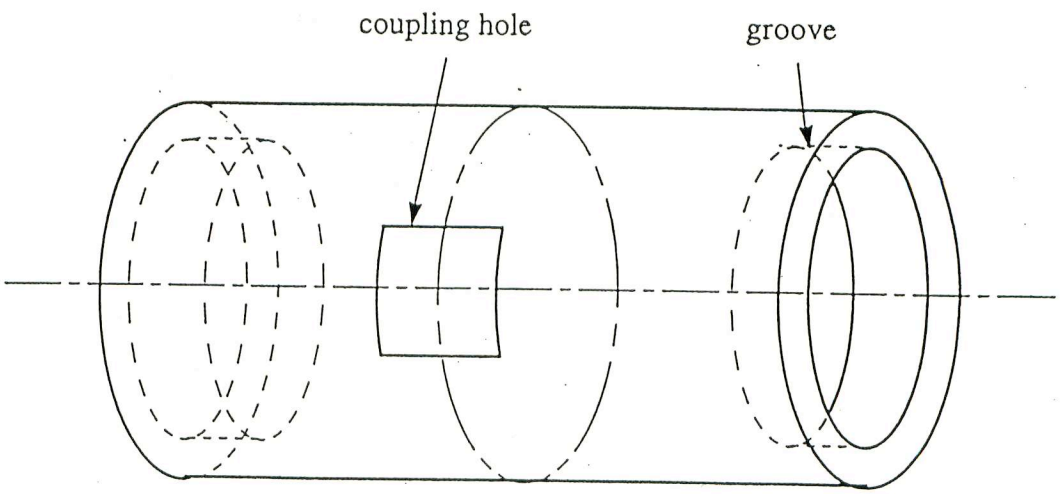

Figure 8.4: Schematic view of the storage cavity.

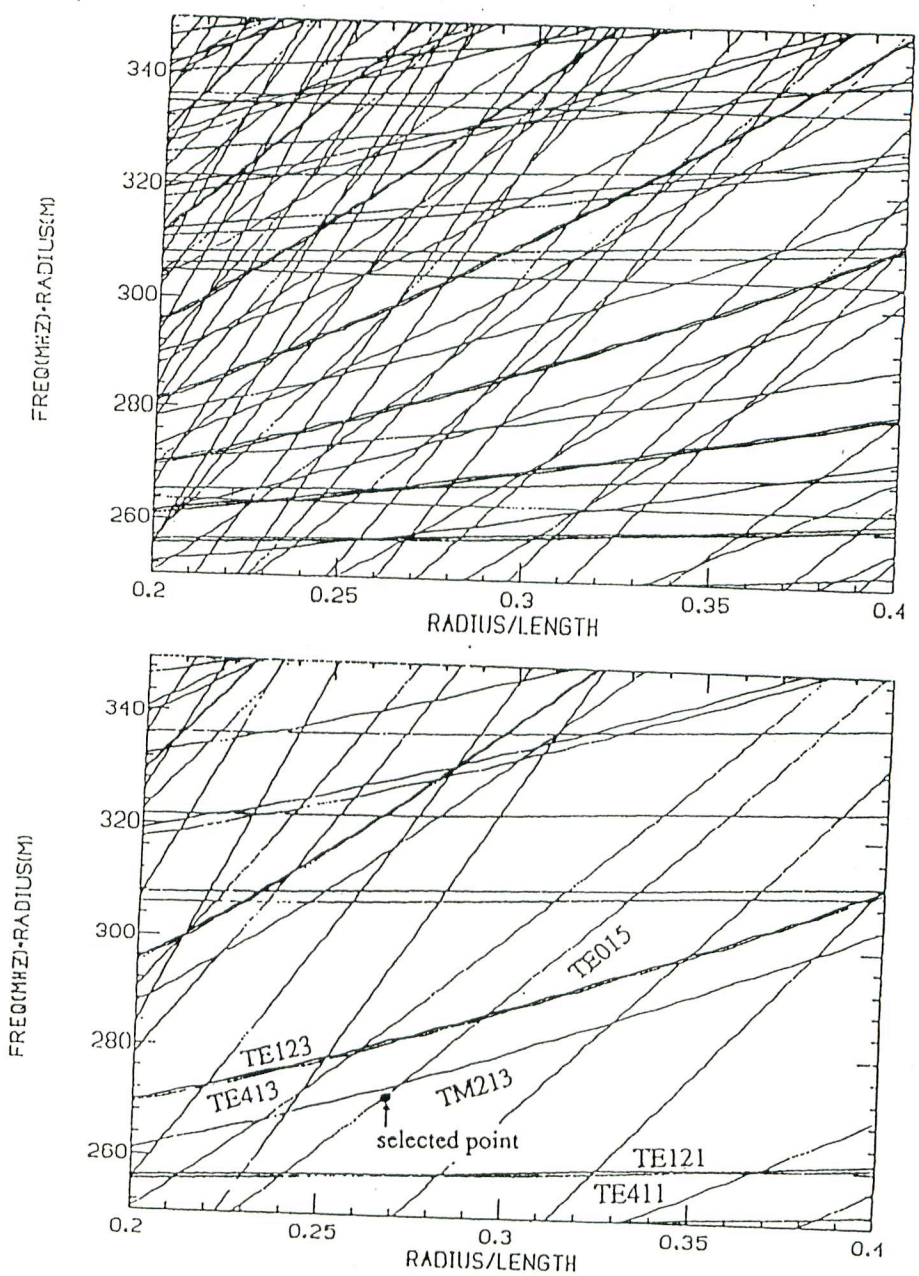

Figure 8.5: Mode diagram in a pillbox cavity. (upper) all TE and TM modes, and (lower) TEmnp (p=odd) and TMmnp ($m > 0$, p=odd) modes.

Table 8.1: Dimensions of the optimized shape.

cavities	accelerating	coupling	storage
radius (mm)	224.0	213.5	535.2
length (mm)	260.0	130.0	1989.4
coupling holes			
location	between a- and c-		between s- and c-
length (mm)	130.0		200.0
width (mm)	180.0		130.0
distance (mm)	0.0		0.0

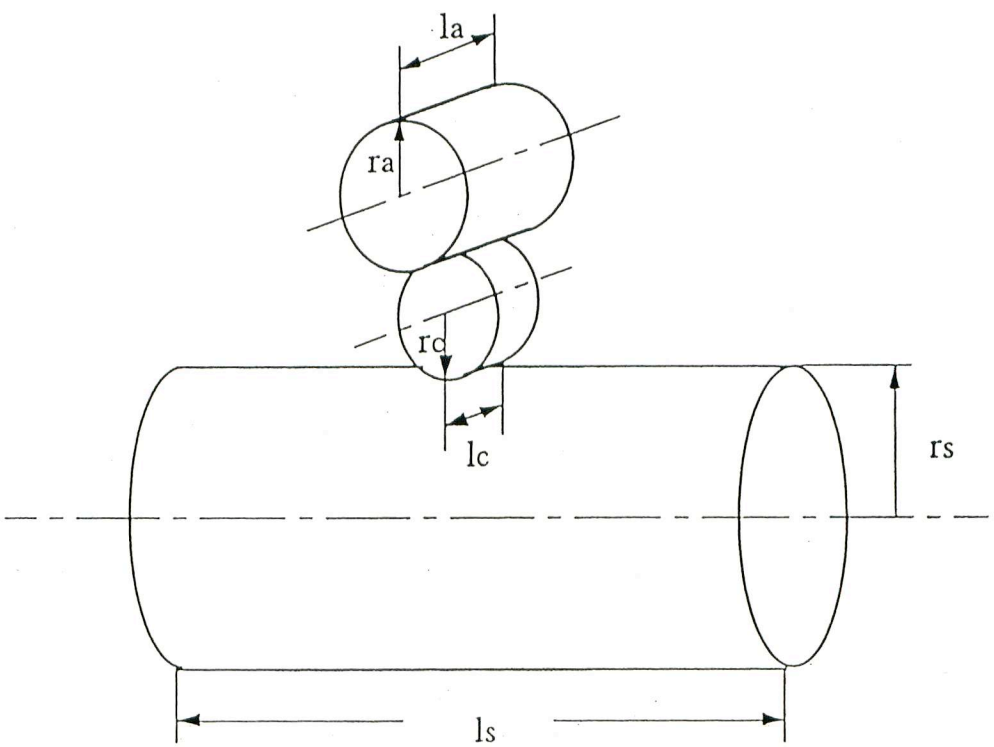

Figure 8.6: Schematic view of the three cavity system.

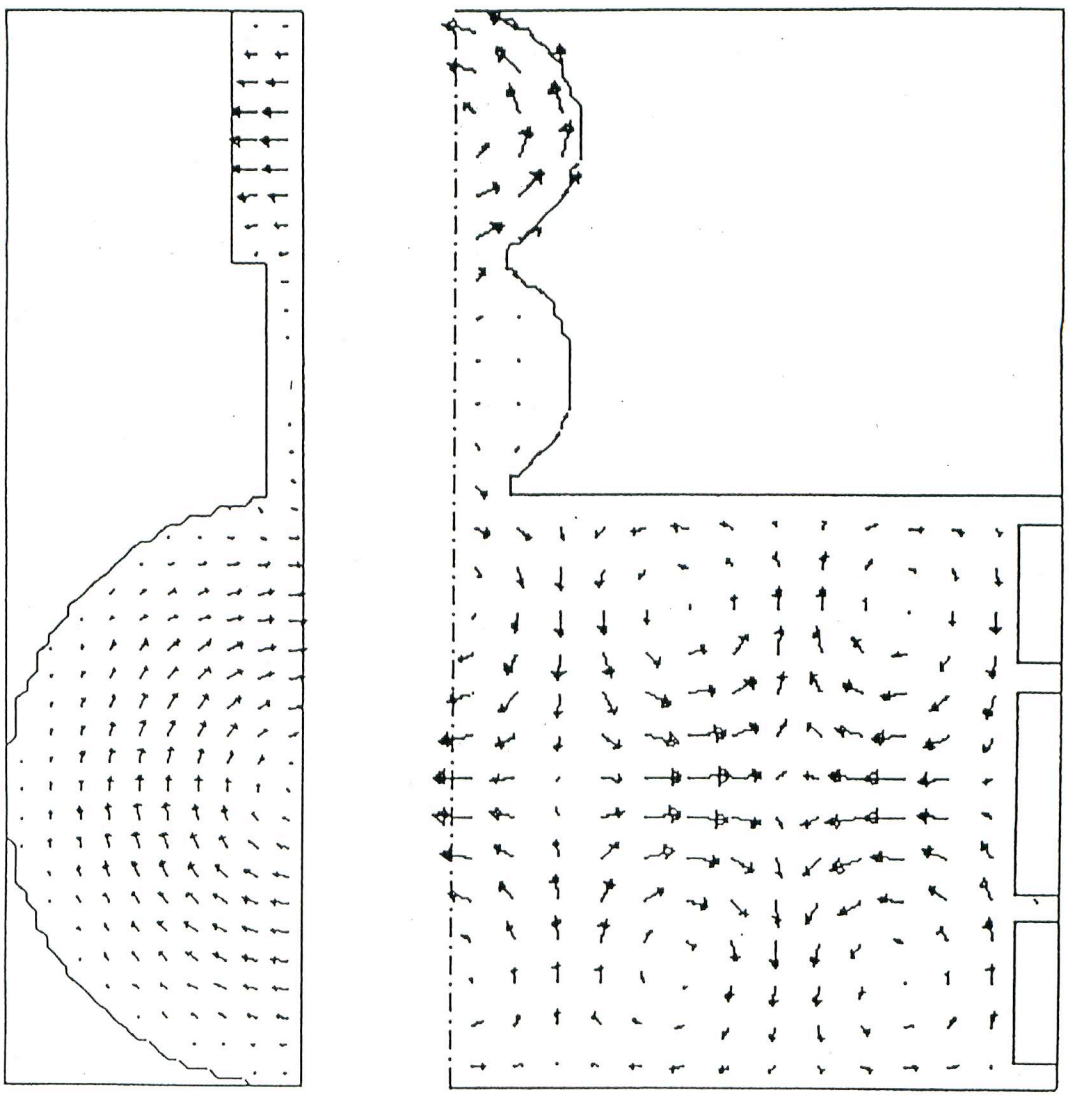

Figure 8.7: Field pattern of the $\pi/2$ mode calculated with the MAFIA code. The electric field (left) and the magnetic field (right) patterns are shown.

$\pi/2$ mode

$f = 508$ MHz

$Q_0 = 1.8 \times 10^5$

$R/Q = 13.9$ Ω

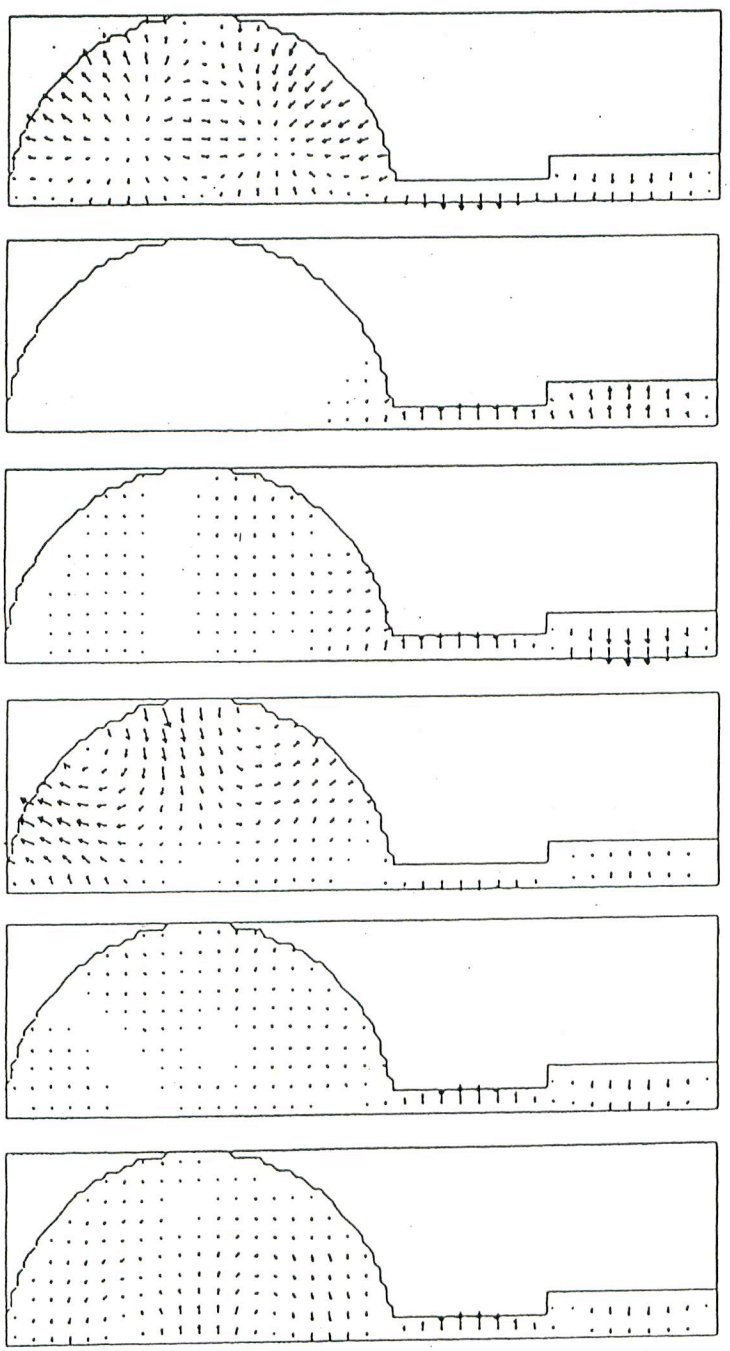

Figure 8.8: Field patterns of the parasitic modes, with frequencies close to the operating mode.

Table 8.2: Properties of the optimized design.

operating mode (TE015, $\pi/2$)				
	frequency	(MHz)	508	
	Q_{total}		1.8×10^5	
	R/Q_{total}	(Ω)	13.9	
	ka		5.6 %	
	ks		1.0 %	
parasitic modes				
TEmnp (p=odd), TMmnp (m>0, p=odd)				
	frequency (MHz)	mode in s-cav.	R/Q_{total} (Ω)	
	474.0	TE411	0.12	
	479.5	TE121	0.04	
	491.2	TM115	0.02	
	499.1	TM213	0.75	
	501.7	TE413/TM213	105.	(0 mode)
	512.8	TE413	71.8	(π mode)
	518.3	TE315	1.04	
	521.0	TE413	16.4	
TEmnp (p=even), TMmnp (p=even)				
	472.3	TM212		
	473.4	TE116		
	475.0	TE314		
	492.0	TE412		
	497.2	TE122		
	516.4	TE216/TM214		
	537.3	TE216/TM214		
	537.7	TM116		
TM0np				
	484.3	TM016		
	501.0	TM022		
	522.4	TM023		

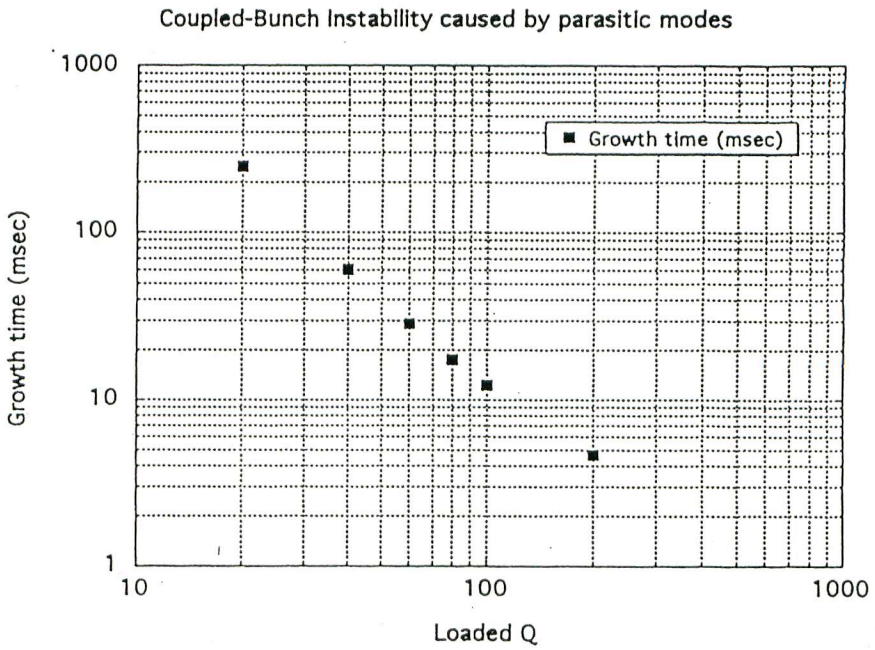

Figure 8.9: Fastest growth time of the coupled bunch instability caused by parasitic modes plotted against the damped Q value.

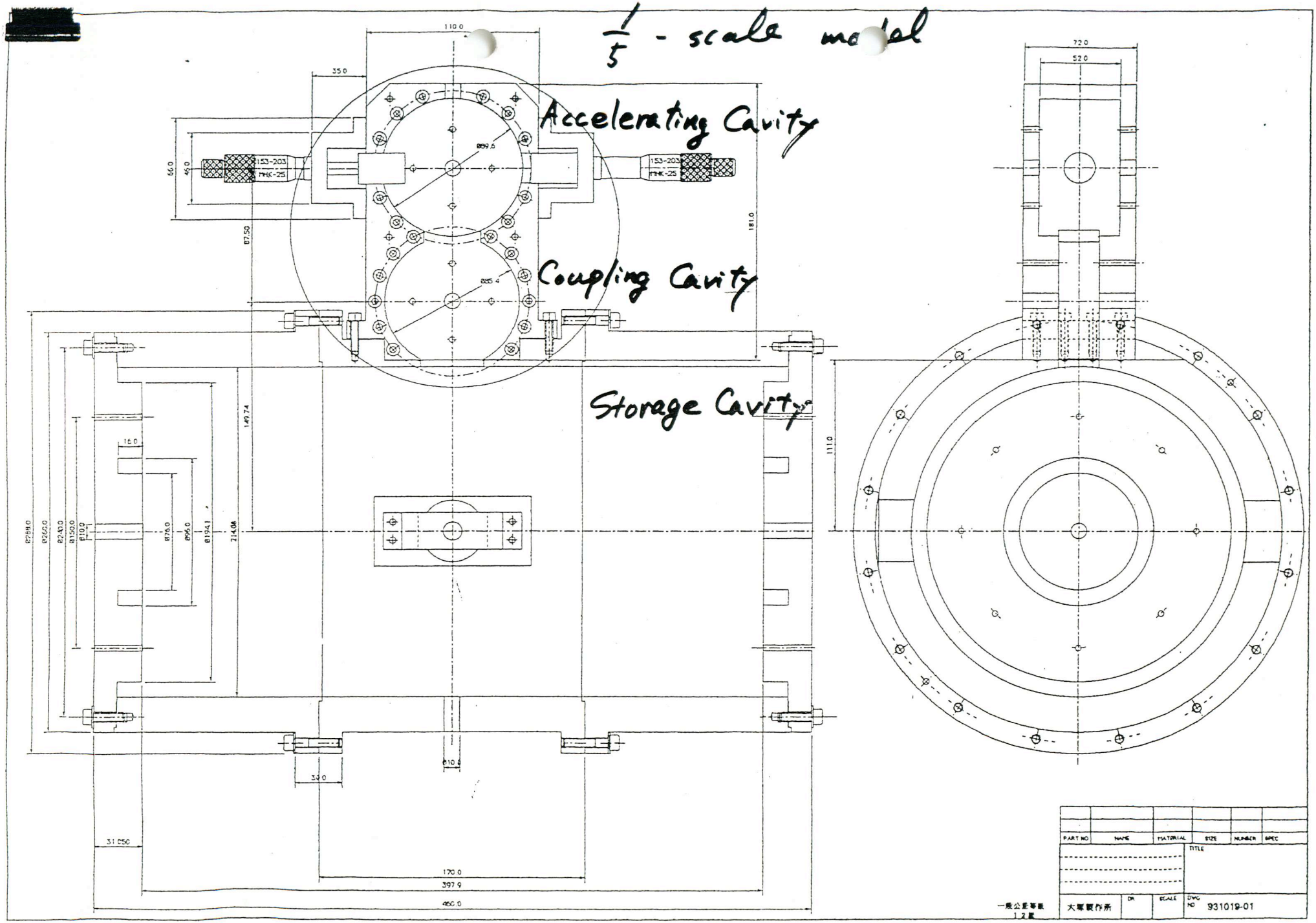
1/5 - scale model
Accelerating Cavity
Coupling Cavity
Storage Cavity
110.0
35.0
66.0
49.0
153-203
TNK-25
87.50
181.0
149.74
214.08
111.0
72.0
52.0
16.0
33.0
31.050
170.0
397.9
466.0
PART NO
NAME
MATERIAL
SIZE
NUMBER
SPEC
TITLE
大塚製作所
SCALE
DWG NO
931019-01

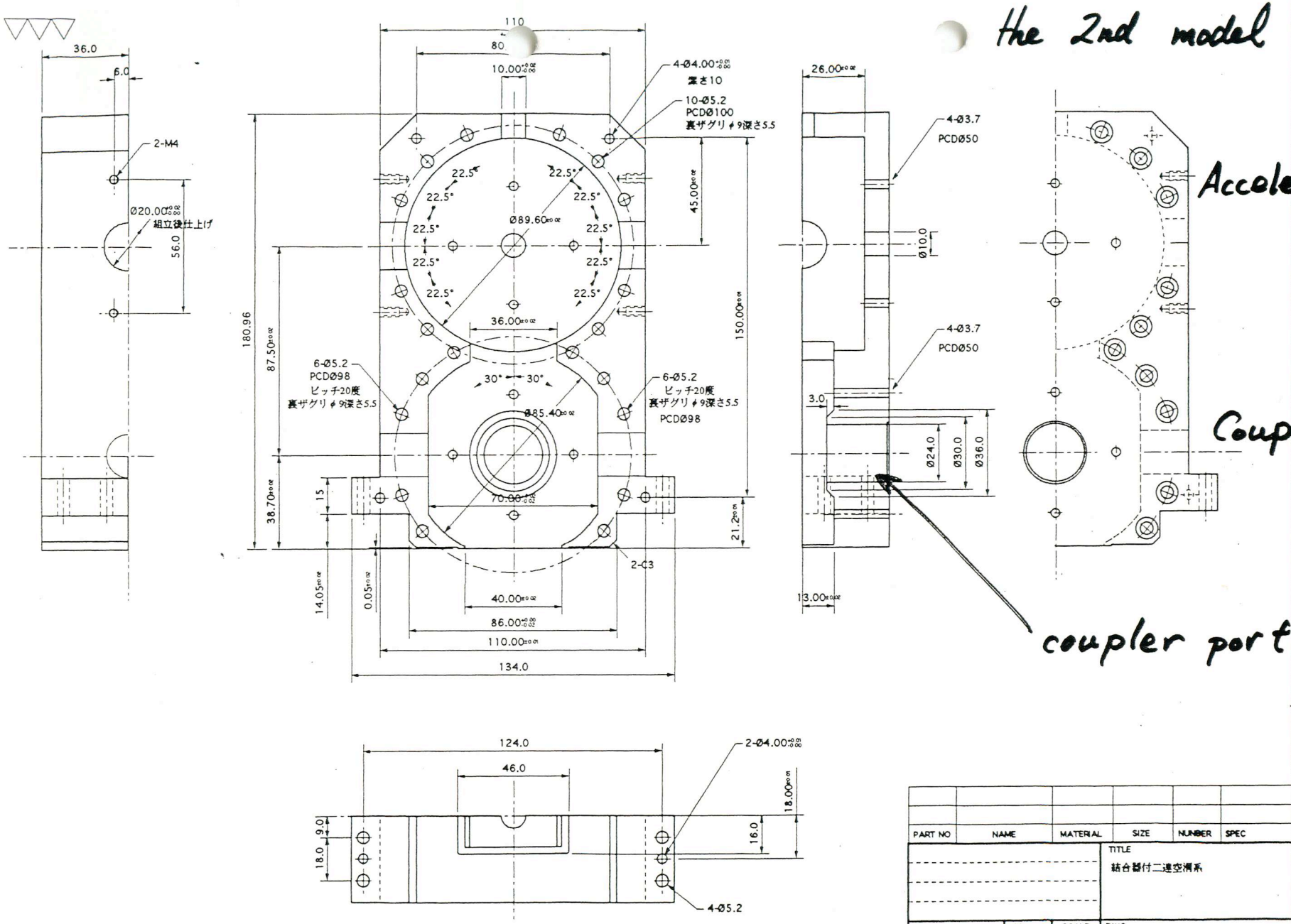
the 2nd model
Accelerating Cavity
Coupling Cavity
coupler port
36.0
6.0
2-M4
Ø20.00
組立後仕上げ
56.0
110
80
10.00
4-Ø4.00
深さ10
10-Ø5.2
PCDØ100
裏ザグリ φ9深さ5.5
22.5°
Ø89.60
45.00
150.00
180.96
87.50
36.00
6-Ø5.2
PCDØ98
ピッチ20度
裏ザグリ φ9深さ5.5
30°
Ø85.40
6-Ø5.2
ピッチ20度
裏ザグリ φ9深さ5.5
PCDØ98
38.70
15
70.00
21.2
2-C3
14.05
0.05
40.00
86.00
110.00
134.0
26.00
4-Ø3.7
PCDØ50
Ø10.0
4-Ø3.7
PCDØ50
3.0
Ø24.0
Ø30.0
Ø36.0
13.00
124.0
46.0
2-Ø4.00
18.00
16.0
9.0
18.0
4-Ø5.2
一般公差等級
12級
PART NO
NAME
MATERIAL
SIZE
NUMBER
SPEC
TITLE
結合器付二連空洞系
DR
SCALE
DWG NO
940407
影山達也

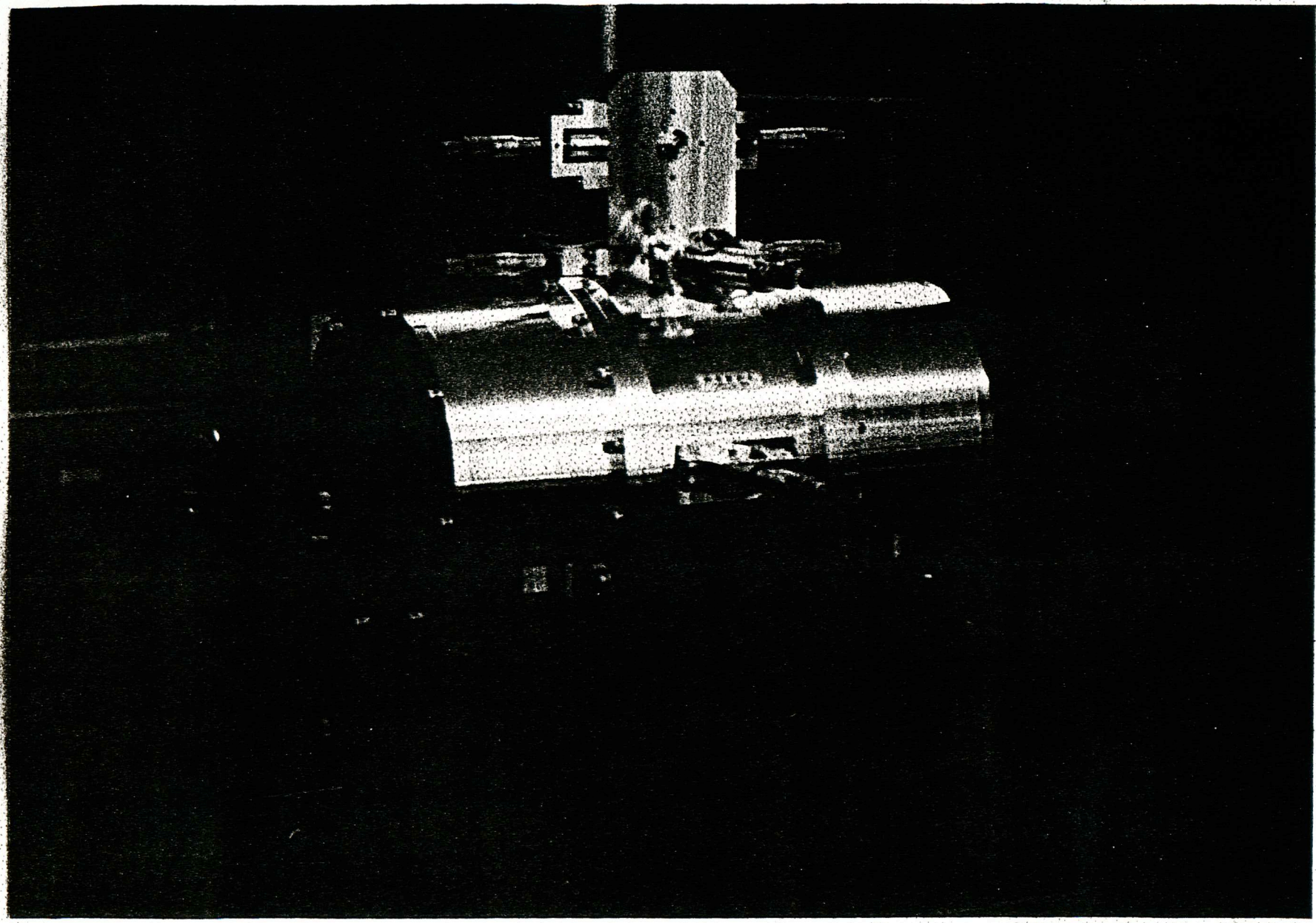

$\frac{1}{5}$ - scale model with couplers

(a) (b)

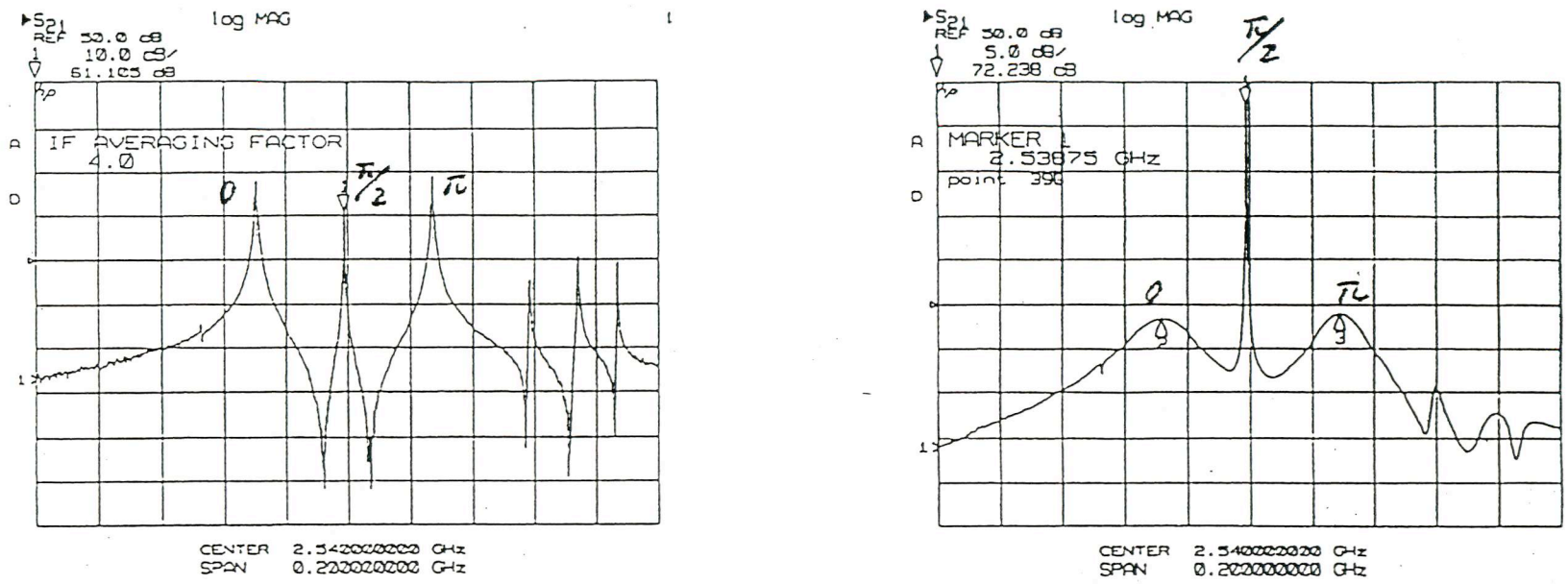

Figure 8.10: Transmission between beam ports: (a) coupling cavity is not damped and (b) is damped.

Table 8.3: Measured parameters of the 0 and π modes.

	f [MHz]	Q	R/Q [Ω]
0 mode	503.4	110	103
π mode	514.9	150	72

$$R \equiv \frac{V^2}{P}$$

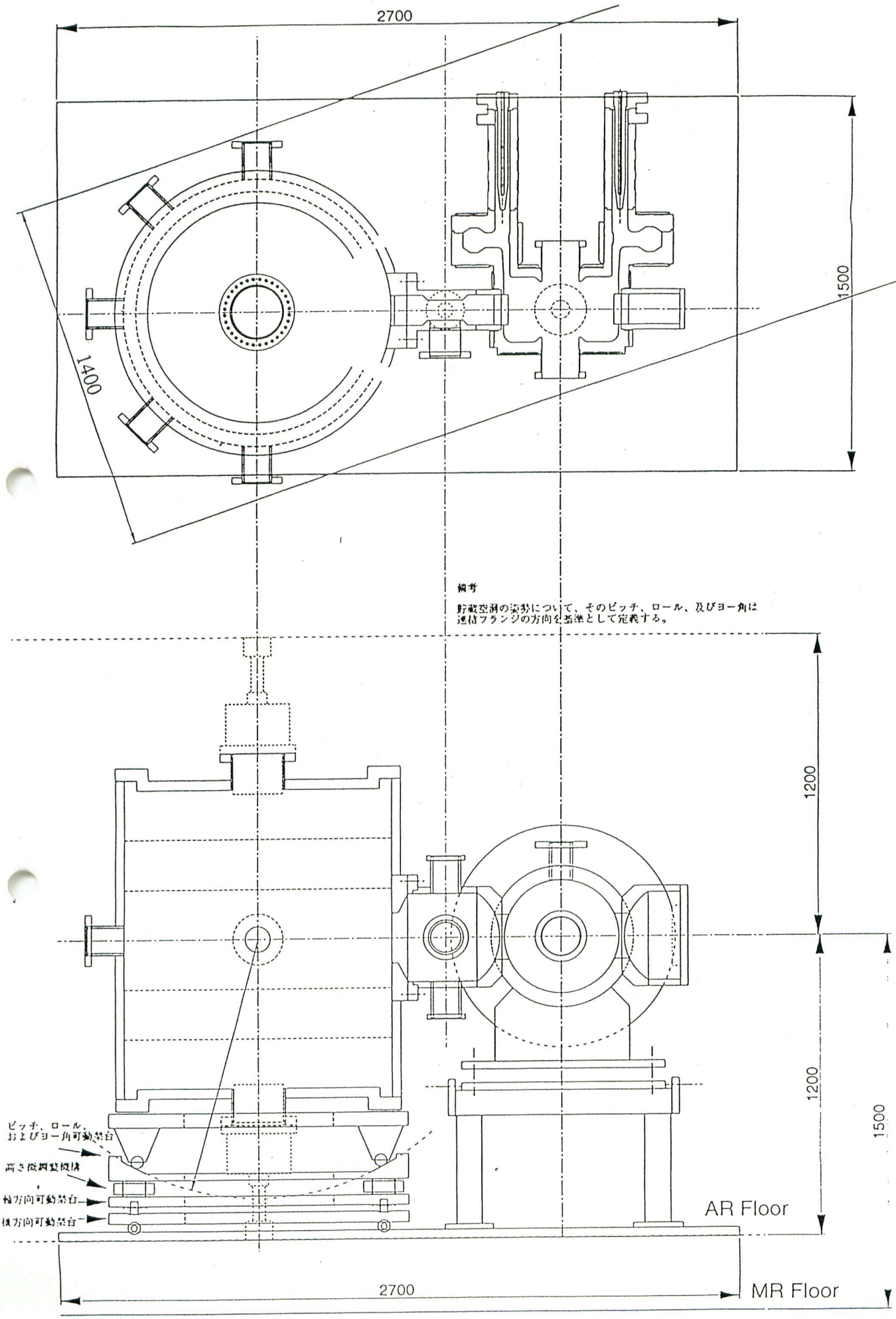

図３　架台構造

ＡＲＥＳ空洞　架台構造
彭山達也　　１９９５年５月２２日

TE013 Storage Cavity 1/1 model

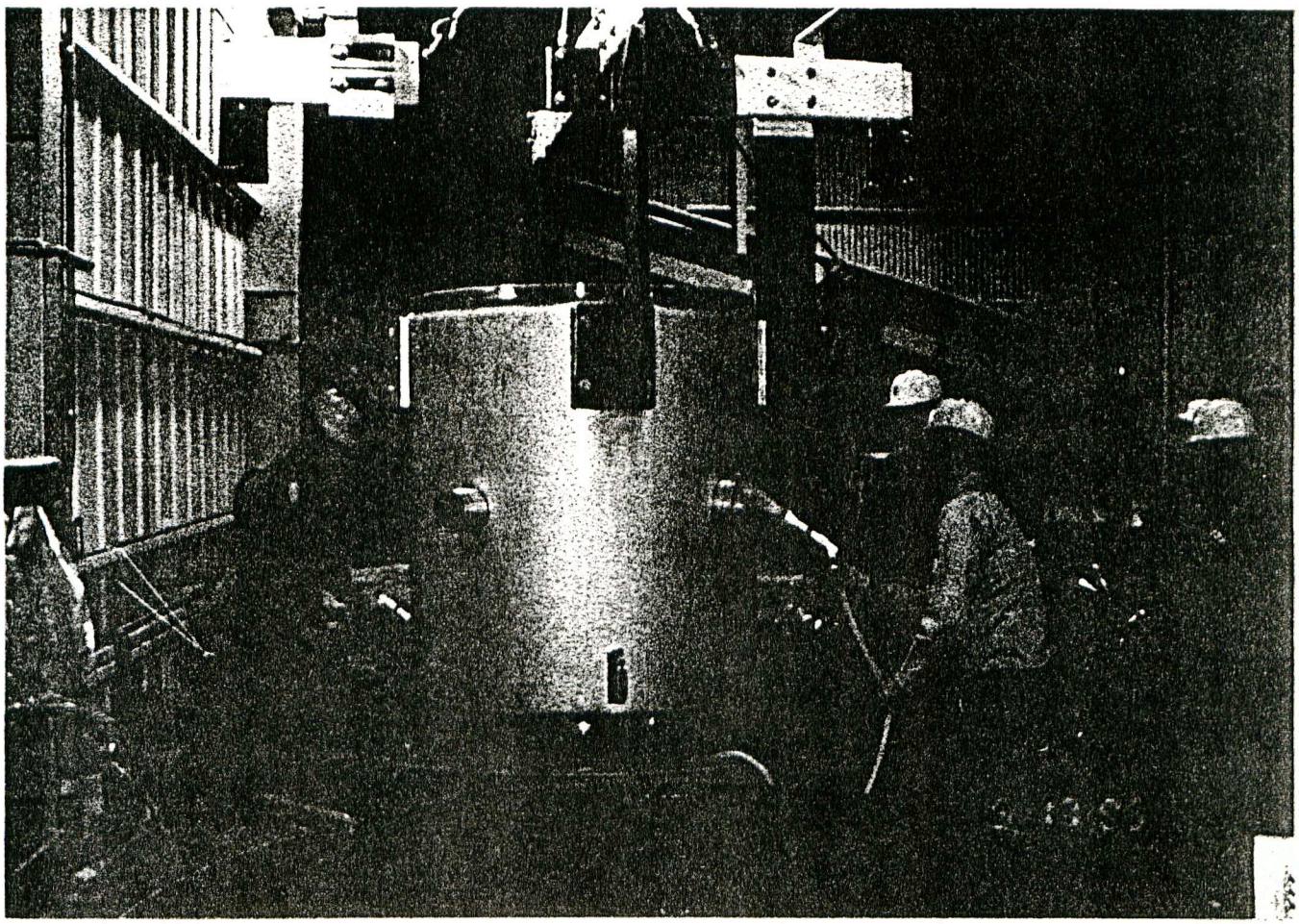

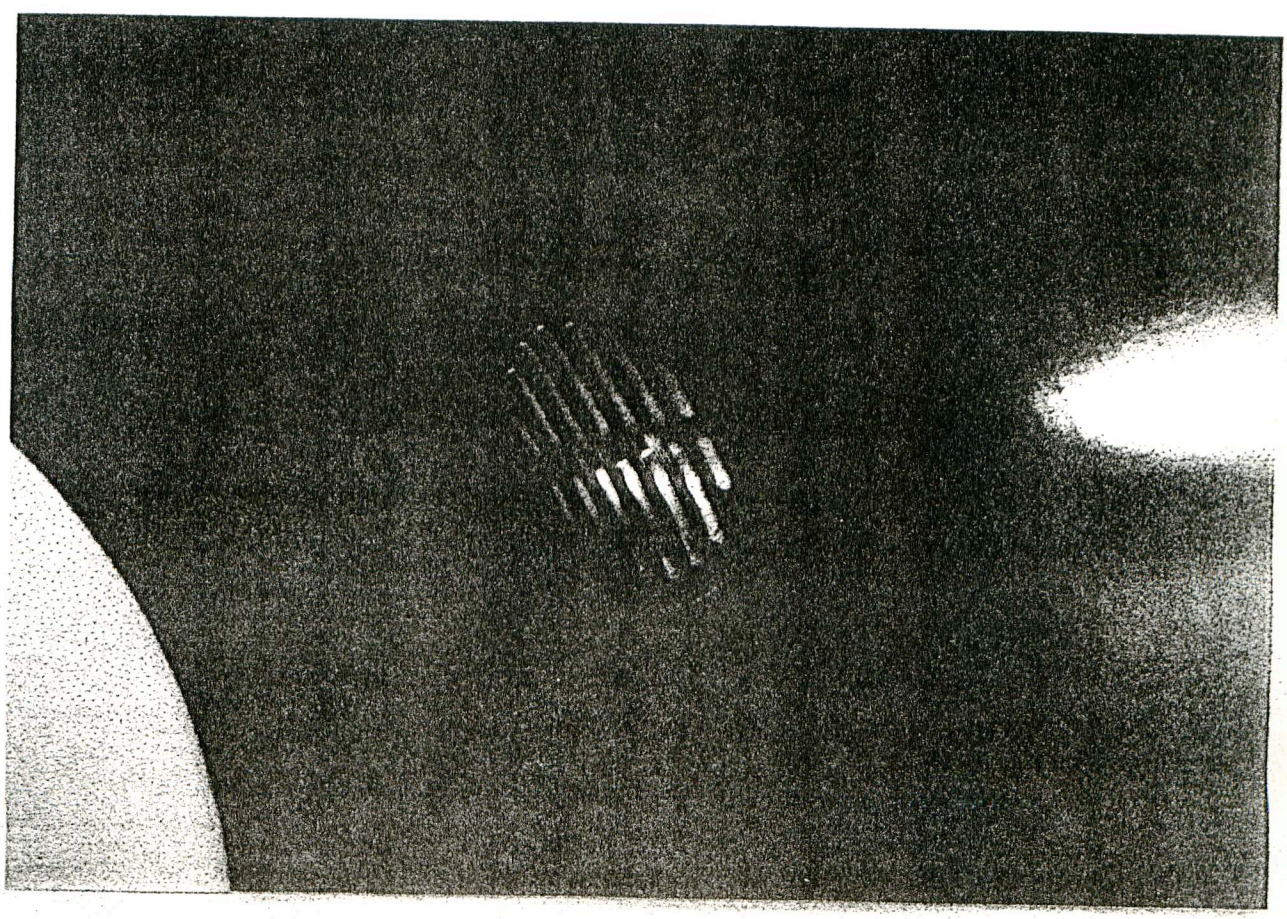

Endplate of the TE013 model cavity

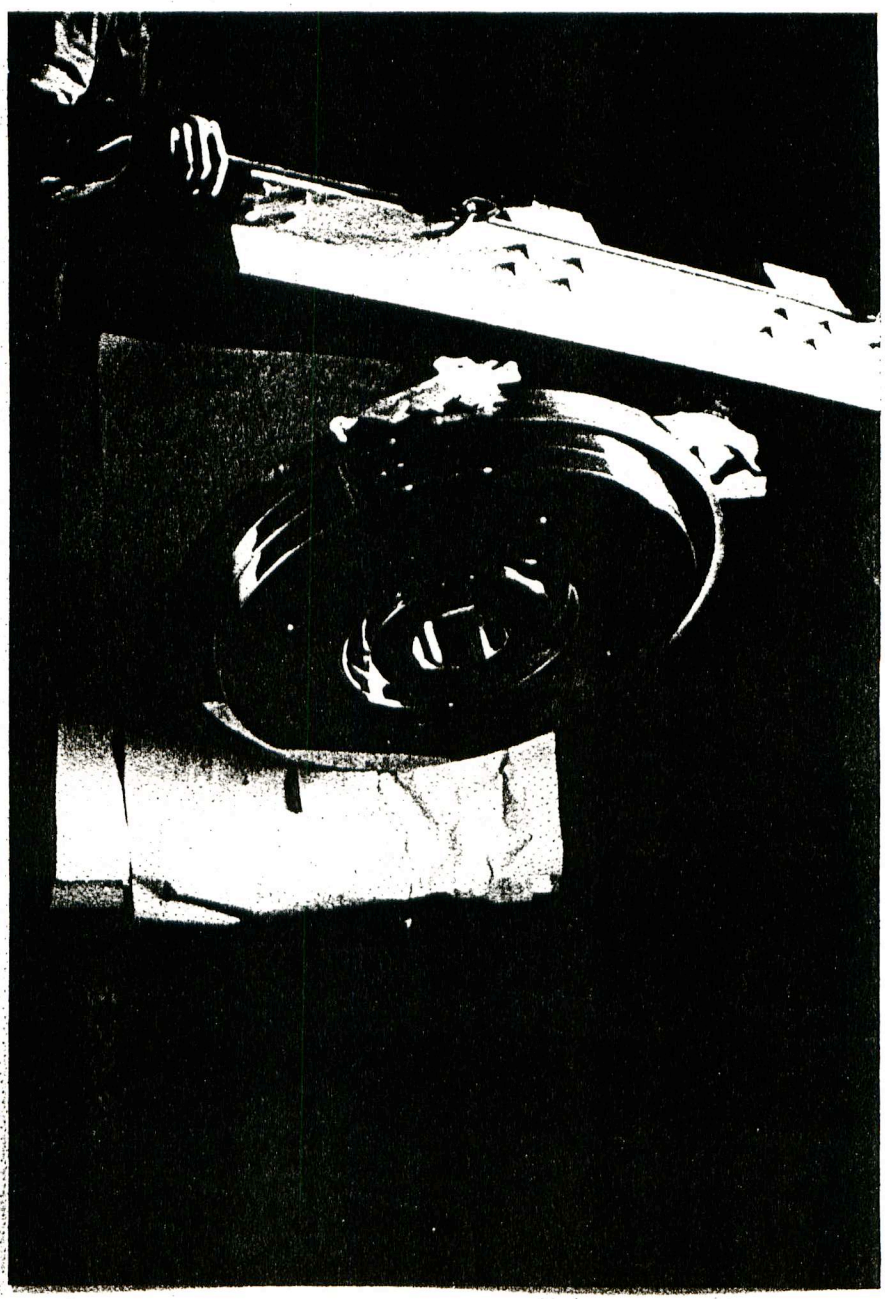

STRUCTURE

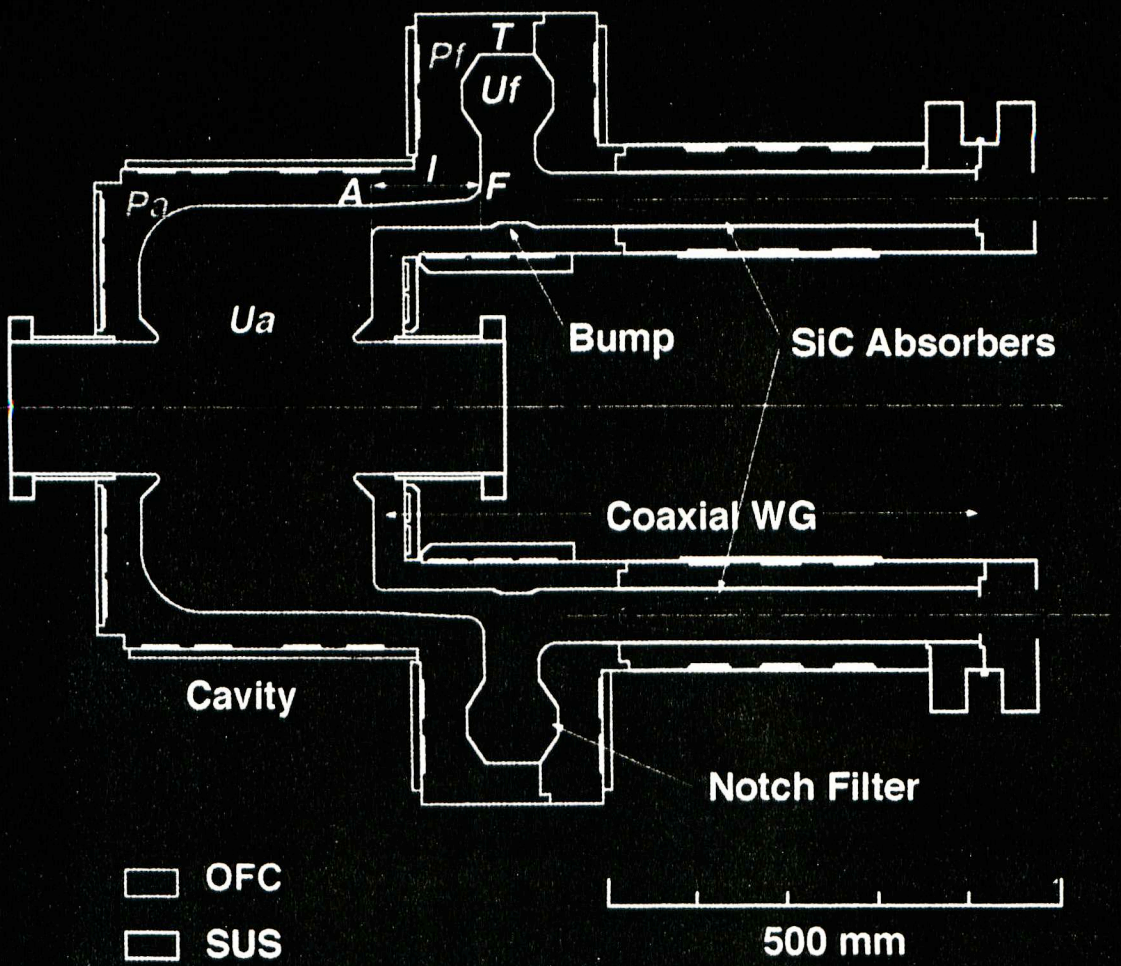

RF parameters of the accelerating mode

f = 508.6 MHz	Vc = 0.6 MV	Pc=75 kW *
R/Q = 150 Ω	Q = 3.2x10^4 *	R = 4.8 MΩ *

* A degradation of ~10% due to copper surface imperfection and the input coupler and tuner ports is taken into account.

Choke-to-Flange Junction from "Microwave Transmission Circuits" Radiation Laboratory Series 1948

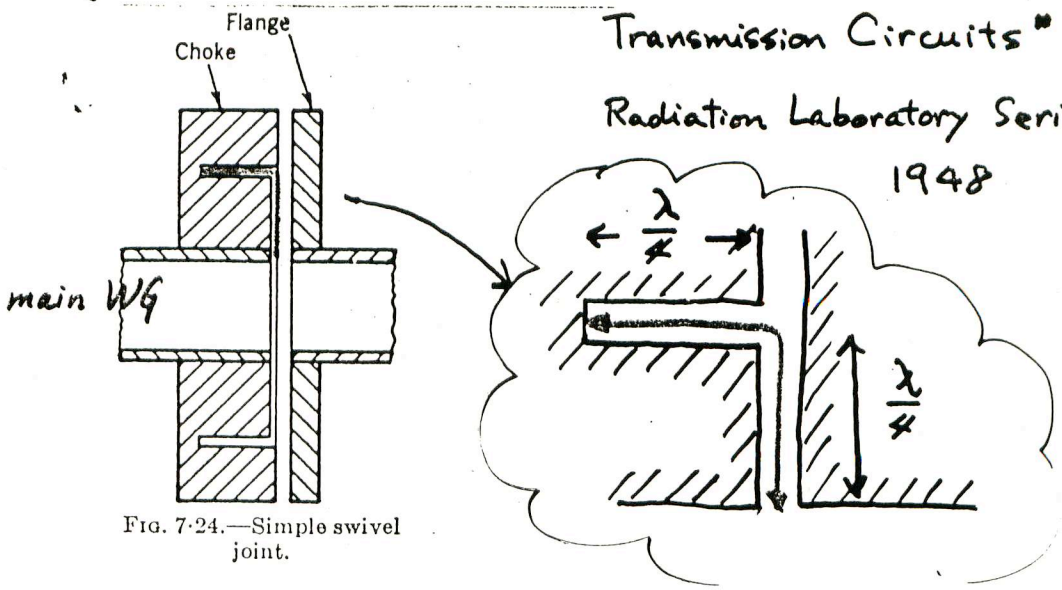

FIG. 7·24.—Simple swivel joint.

a series-branching transmission line of $\frac{\lambda}{2}$

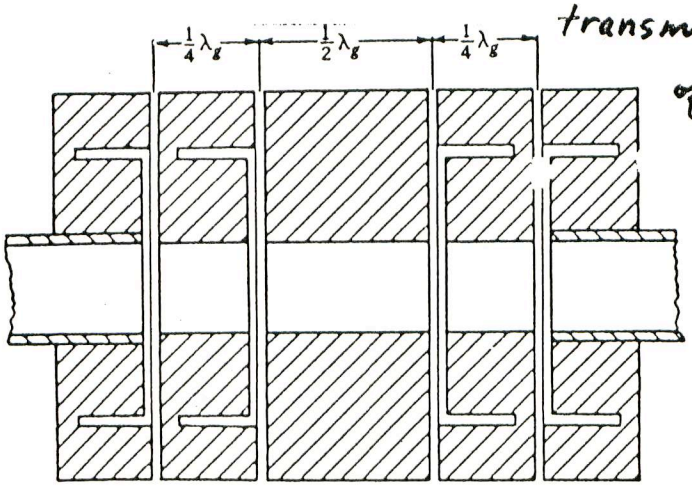

FIG. 7·30.—Four-junction swivel joint.

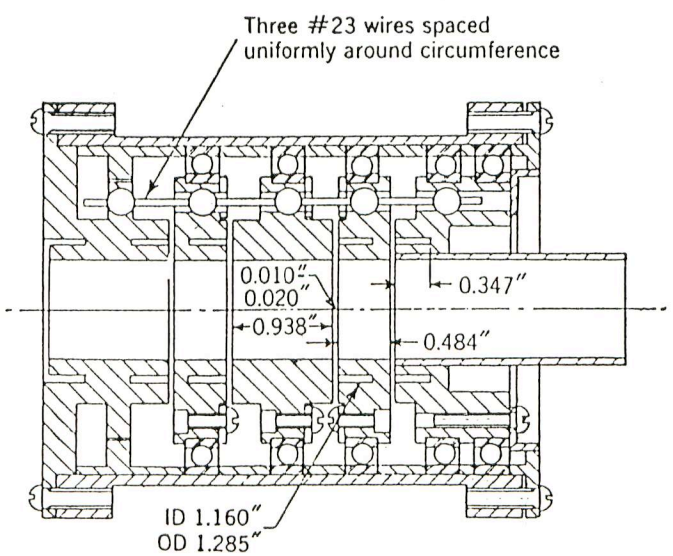

FIG. 7·34.—Construction of the 3-cm four-junction swivel joint.

チョーク型構造

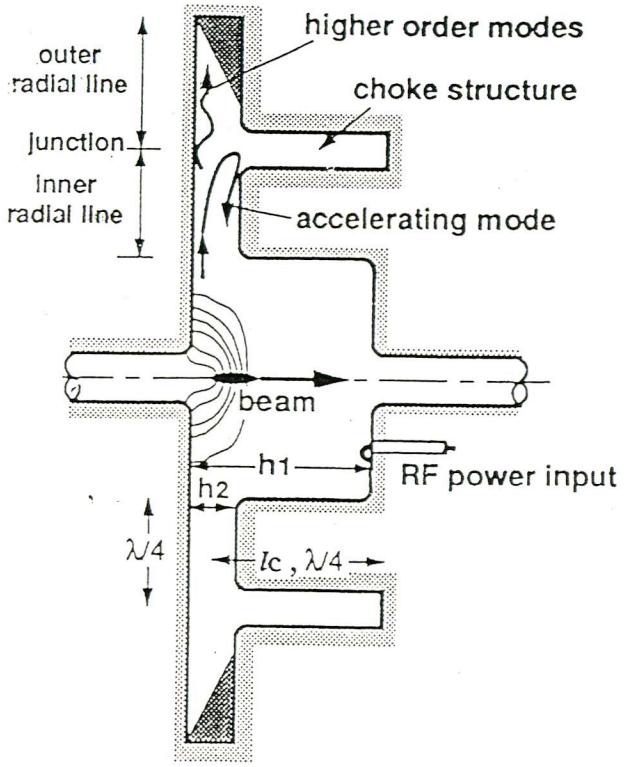

T. Shintake, Jpn. J. Appl. Phys., 31 L1567 (1992)

S-band 加速管

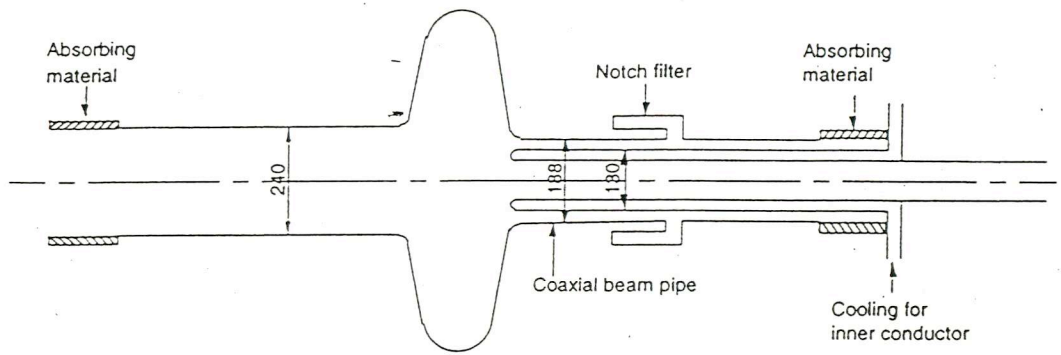

K. Akai et al.,
Proc. B Factories
"The State of the Art in Accelerators, Detectors and Physics",
SLAC, April 6-10, 1992

Crab 空洞
(バンチに偏流修正角を与える.)
Crab angle

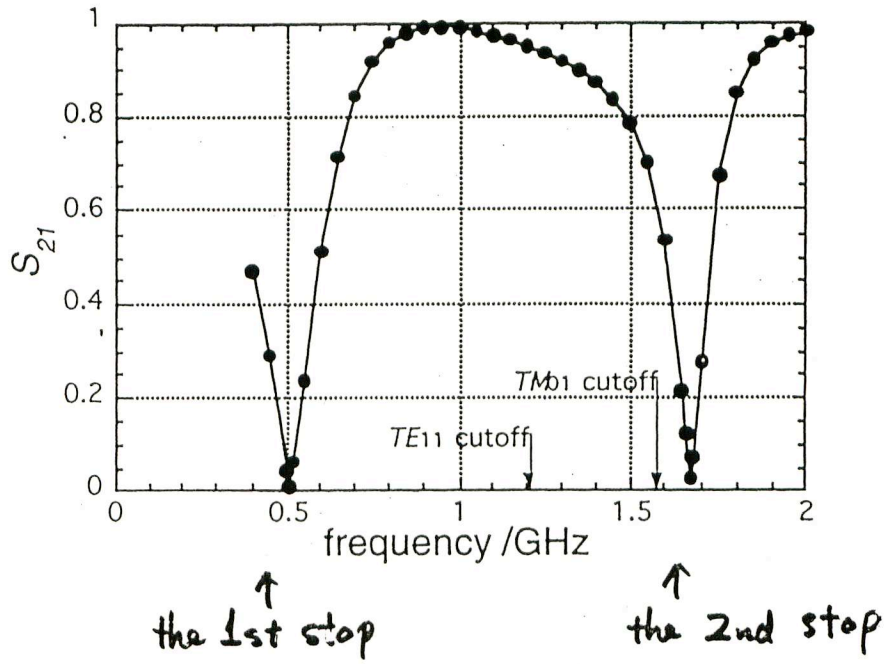

Figure 8.12: The frequency response of S_{21} of the notch filter.

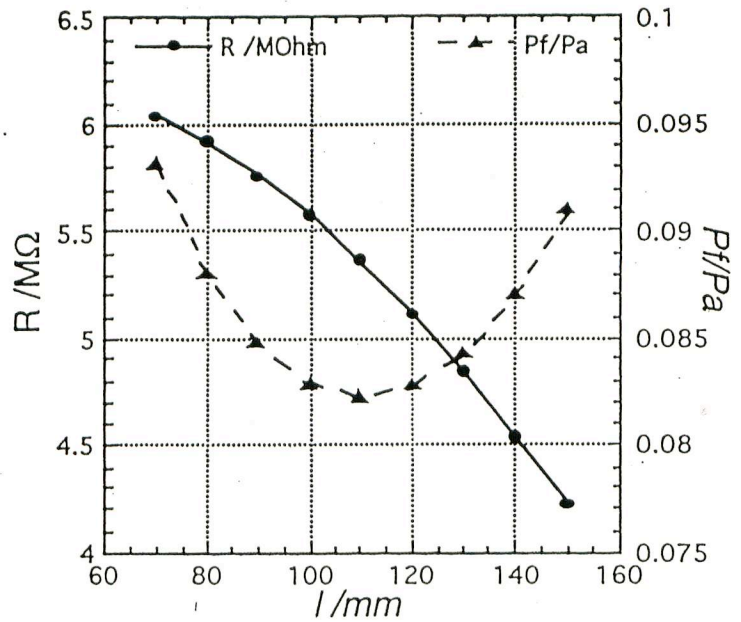

Figure 8.13: The ratio P_f/P_a and the shunt impedance are plotted as a function of l.

Table 8.5: Ring parameters used in the calculation of the growth time of the coupled bunch instability in Figure 8.14(b).

Parameters		
Beam Energy	3.5	GeV
Beam Current	2.6	A
RF Frequency	508.9	MHz
Number of Bunches	5120	
Momentum Compaction	1.5×10^{-4}	
Synchrotron Frequency	1.7	kHz
Number of Cavities	20	

(a) (b)

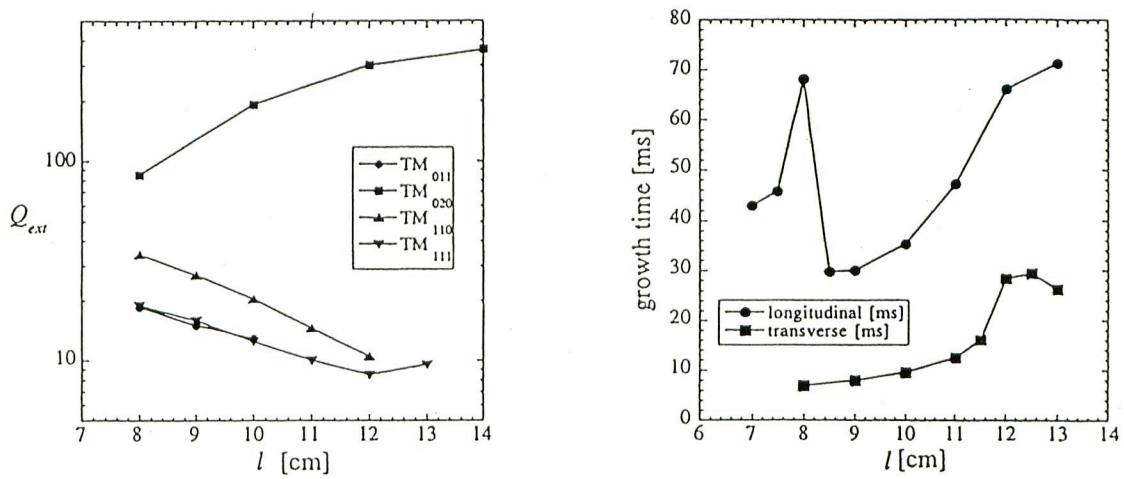

Figure 8.14: (a) Q_{ext} and (b) growth time of coupled bunch instability as a function of the length between the cavity and notch filter l.

Table 8.6: HOM impedances of the accelerating cavity of the ARES.

monopole			
f(MHz)	$R/Q(\Omega)$	Q_L	$(R/Q) \times Q_L$ (Ω)
76.2	17.4	71.5	1243
190	4.5	24.5	109
662.6	2.8	25.4	72.2
731.7	11.0	35.7	394
821.8	7.9	22.7	180
925.2	3.8	16.6	62.4
1331.9	3.2	28.7	90.7
1389.5	3.1	27.8	86.4
dipole			
f(MHz)	R/Q (Ω/m)	Q_L	$(R/Q) \times Q_L$ $(k\Omega/m)$
275.4	50.7	63.4	3.21
670.0	16.6	37.1	0.62
766.2	167	50.9	8.51
826.7	113	30.4	3.43
905.8	109	20.5	2.23
986.8	210	23.2	4.85
1067.5	68.1	10.4	0.70

1

溫度分布

Temperature Contour Plot

($P_c = 90 kW$)

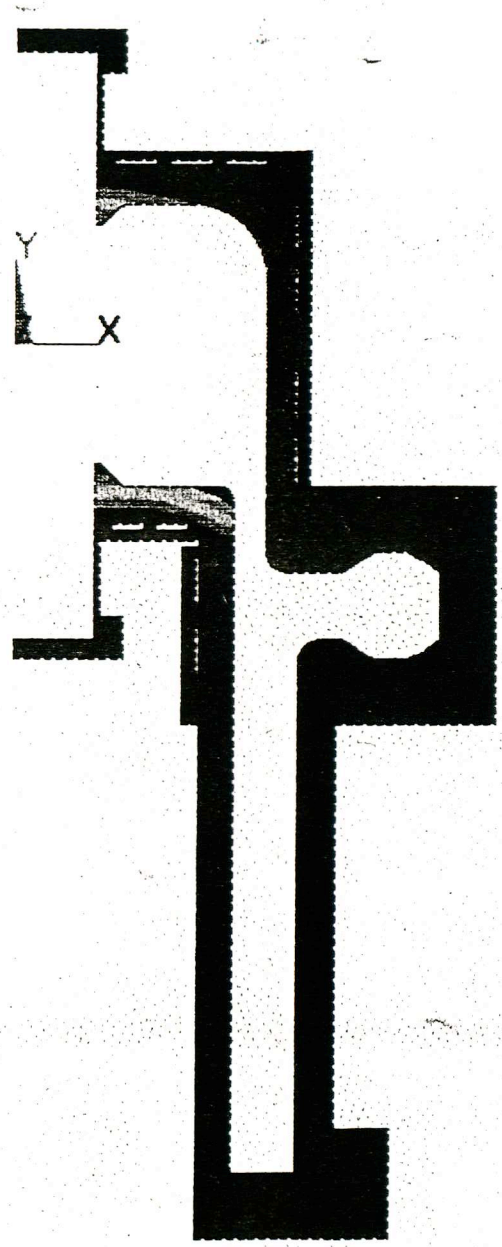

DEC 5, 1993
0:45:48
NODAL SOLUTION
STEP=1
SUB =1
TIME=1
TEMP
TEPC=.224144
SMN =303.345
SMX =327.122

303.345
305.987
308.629
311.271
313.913
316.555
319.197
321.838
324.48
327.122

in Kelvin

TR2C thrml-strctrl analysis

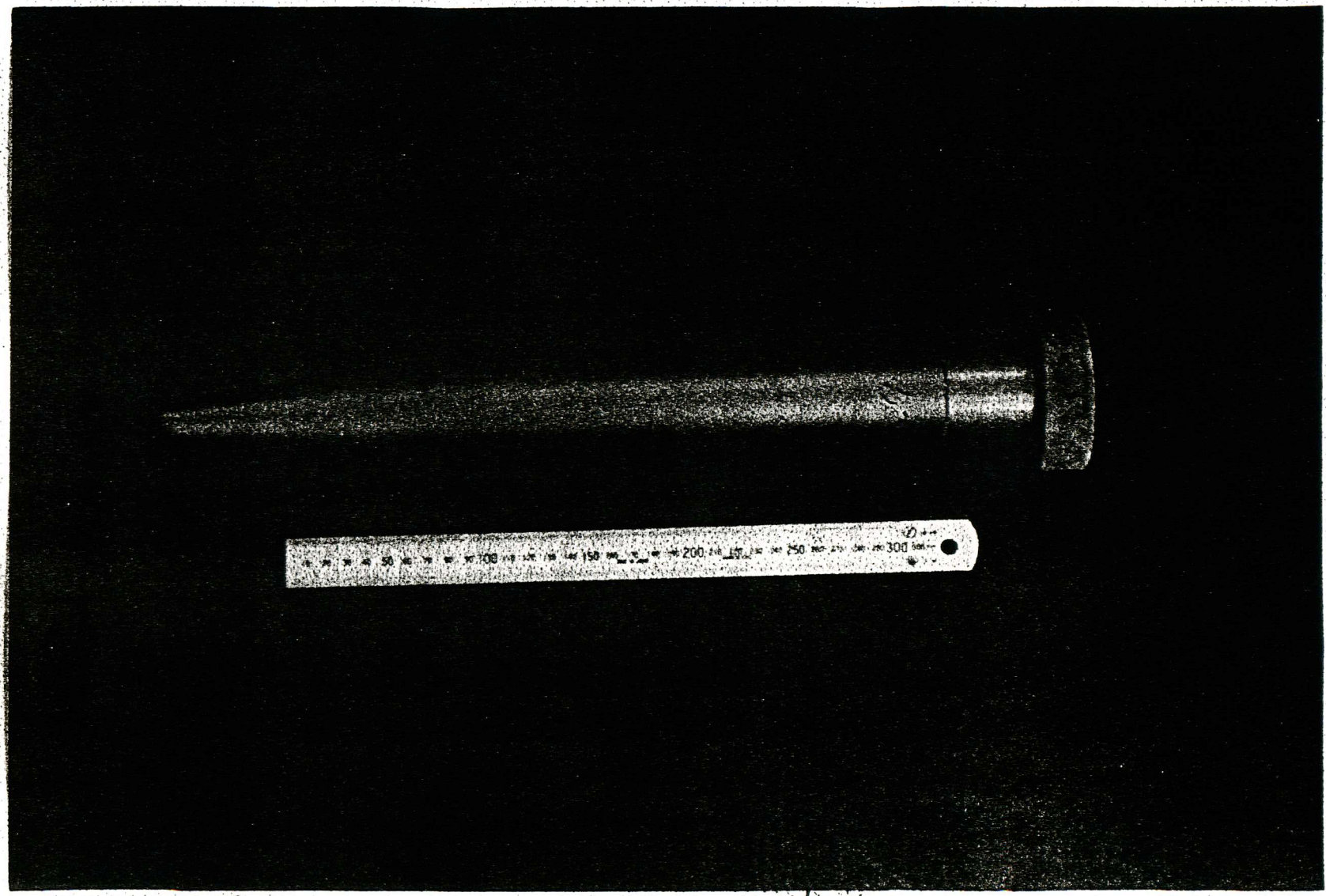

1 SiC absorber { Φ 40 mm
L = 400 mm

SiC absorber

$$\varepsilon = \varepsilon' - j\varepsilon'' \qquad \tan\delta = \frac{\varepsilon''}{\varepsilon'}$$

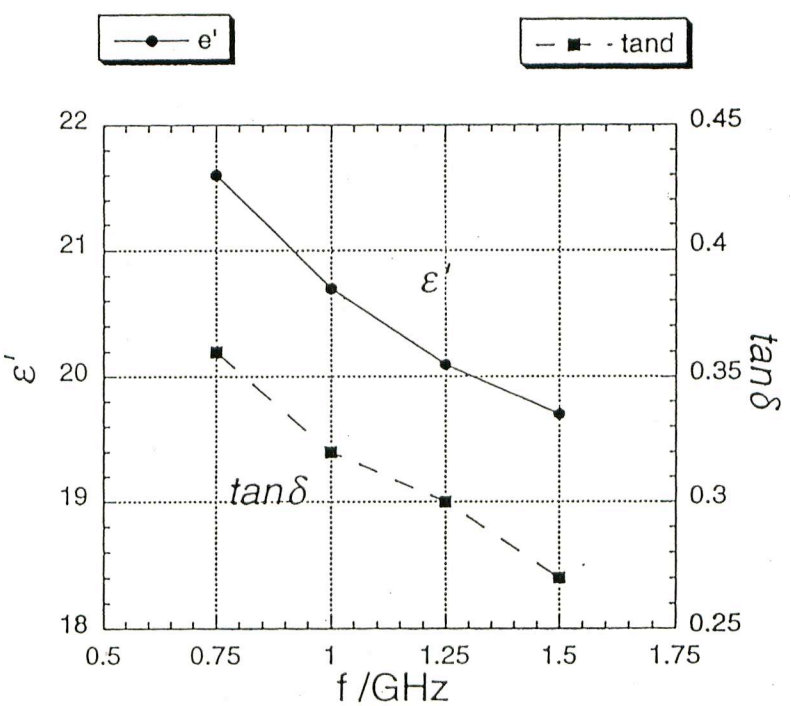

Figure 8.16: The dielectric constant and loss tangent of the SiC ceramics are plotted as a function of frequency.

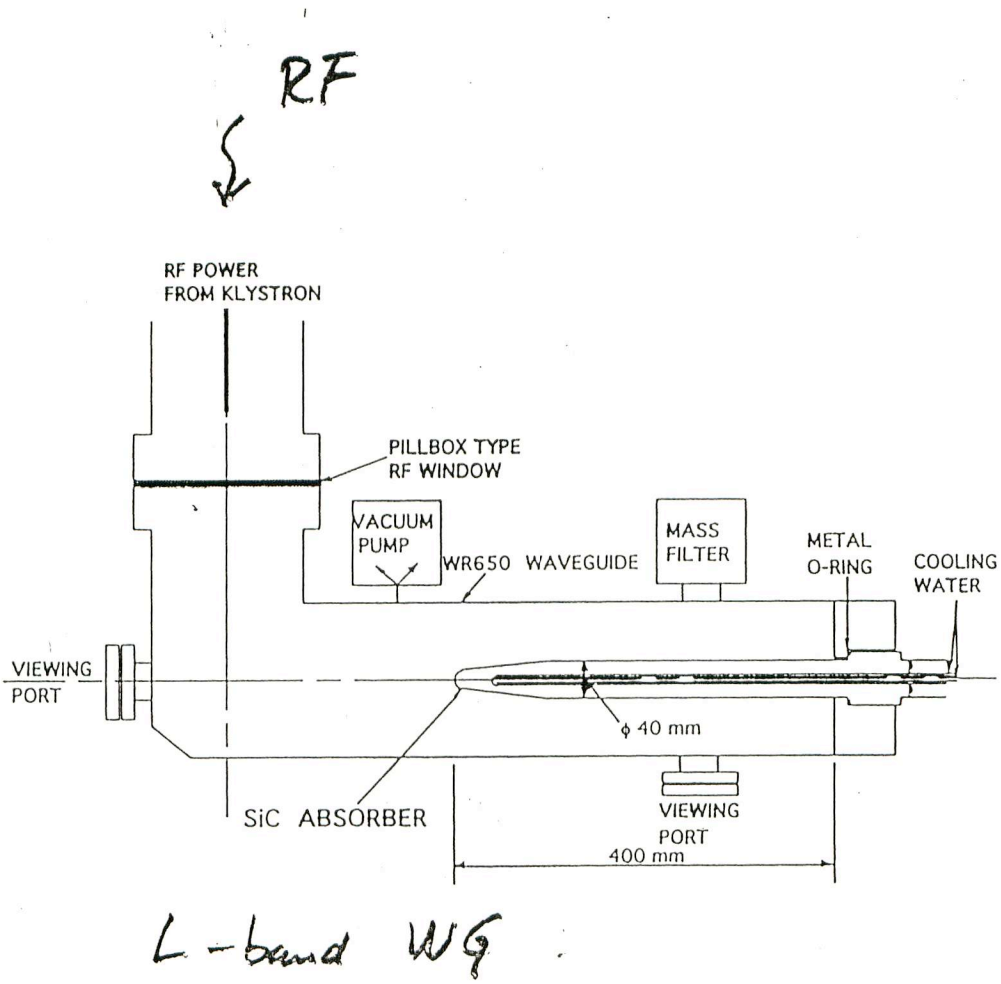

Figure 8.17: The layout of the high power test.

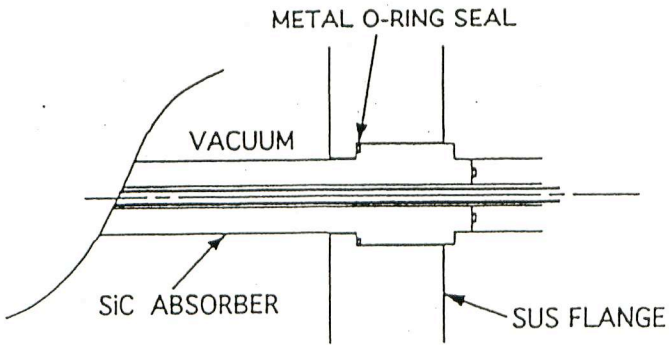

Figure 8.18: A prototype of the SiC absorber using a metal O-ring for vacuum seal.

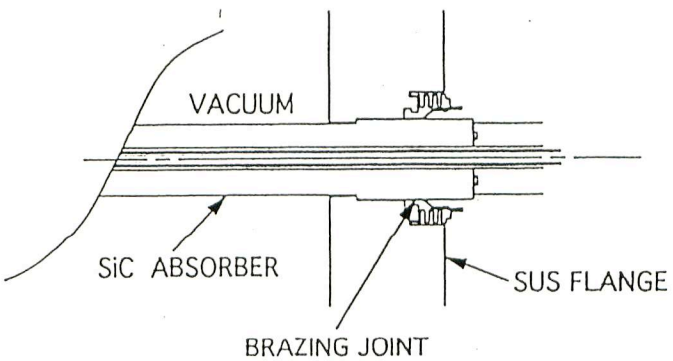

Figure 8.19: The next prototype of the SiC absorber using a brazing joint. The SiC ceramics is directly brazed to the copper sleeve.

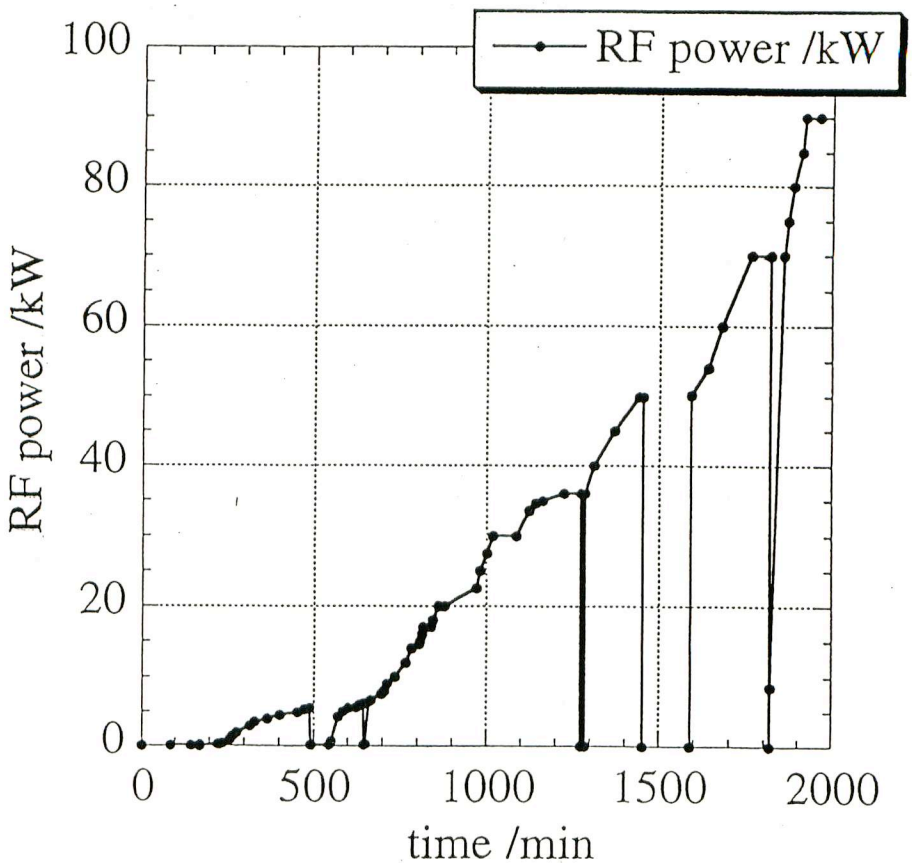

History of RF conditioning
of the high-power HOM-damped cavity

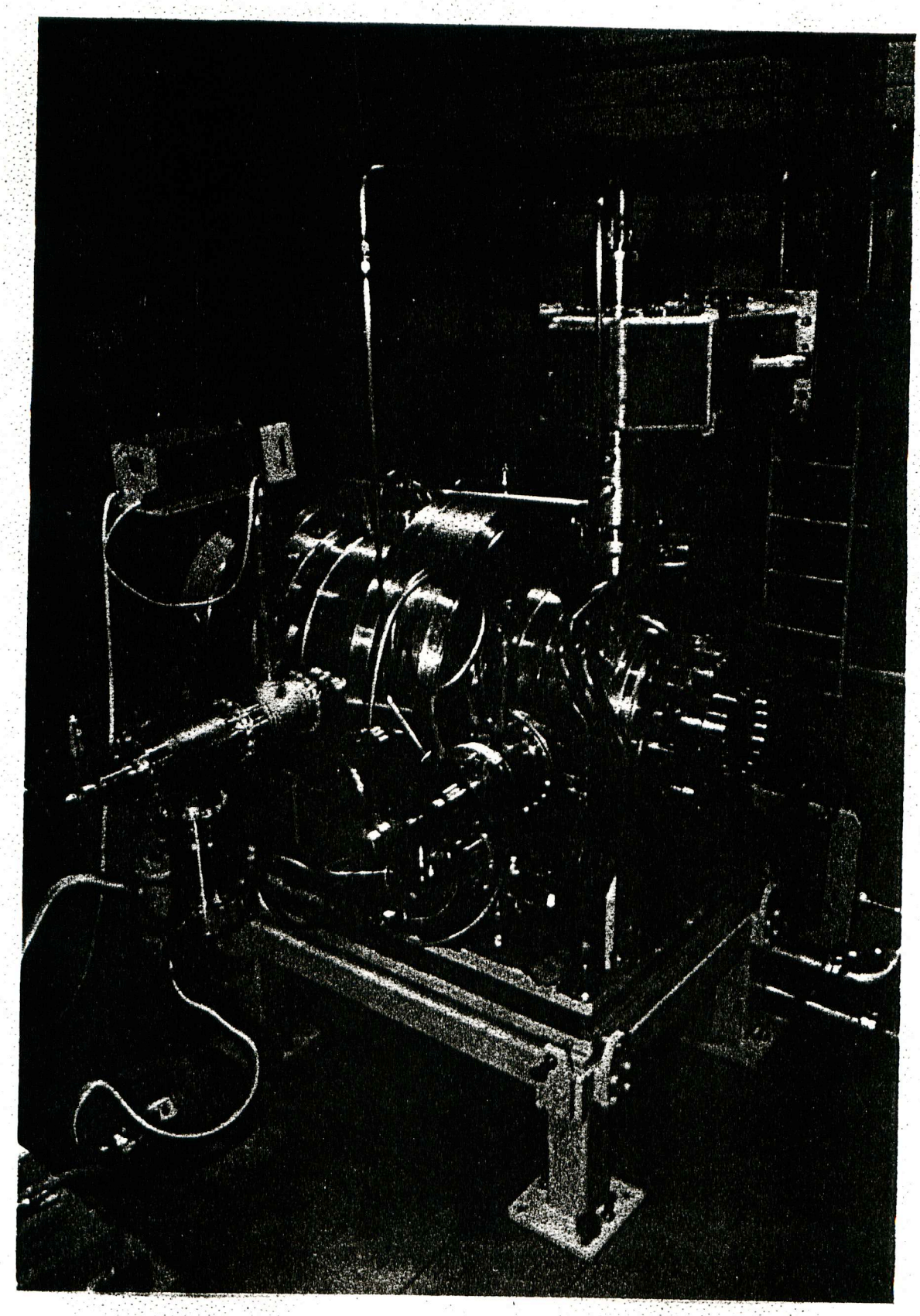

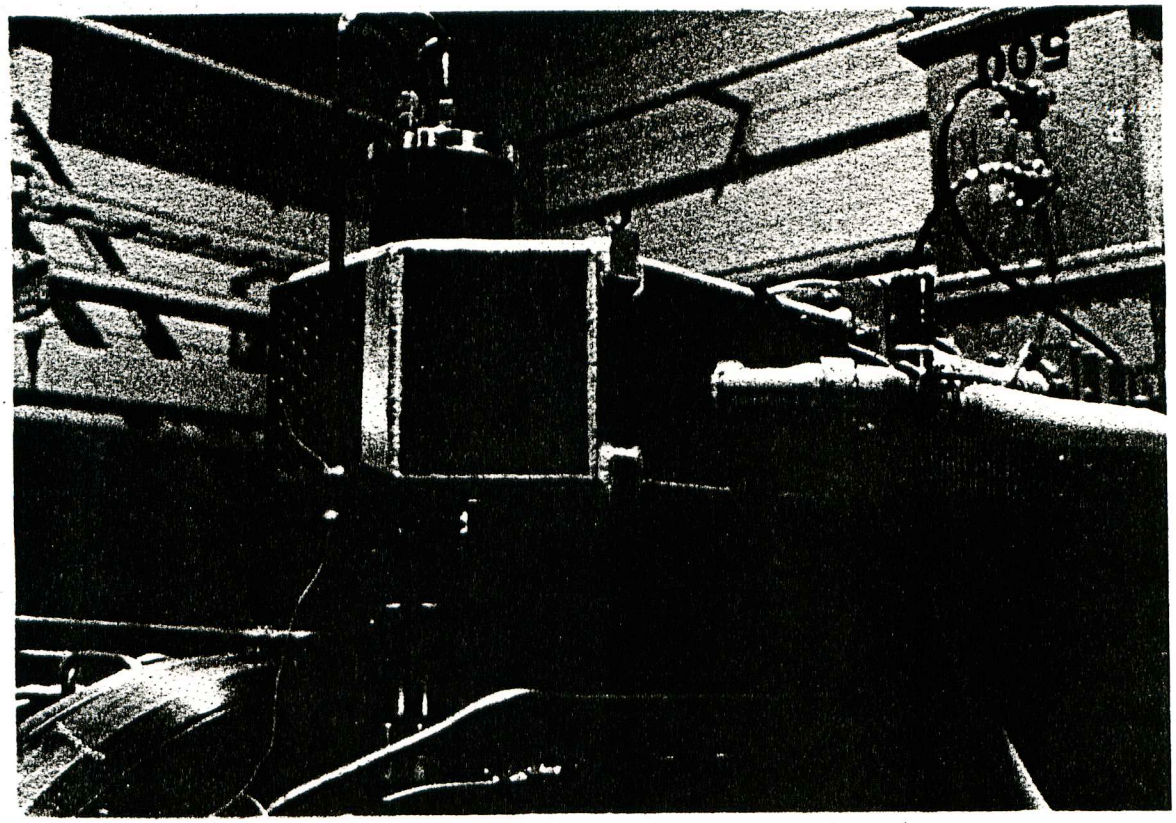

Input Coupler (TRISTAN APS Cavity
P ≃ 300 KW)

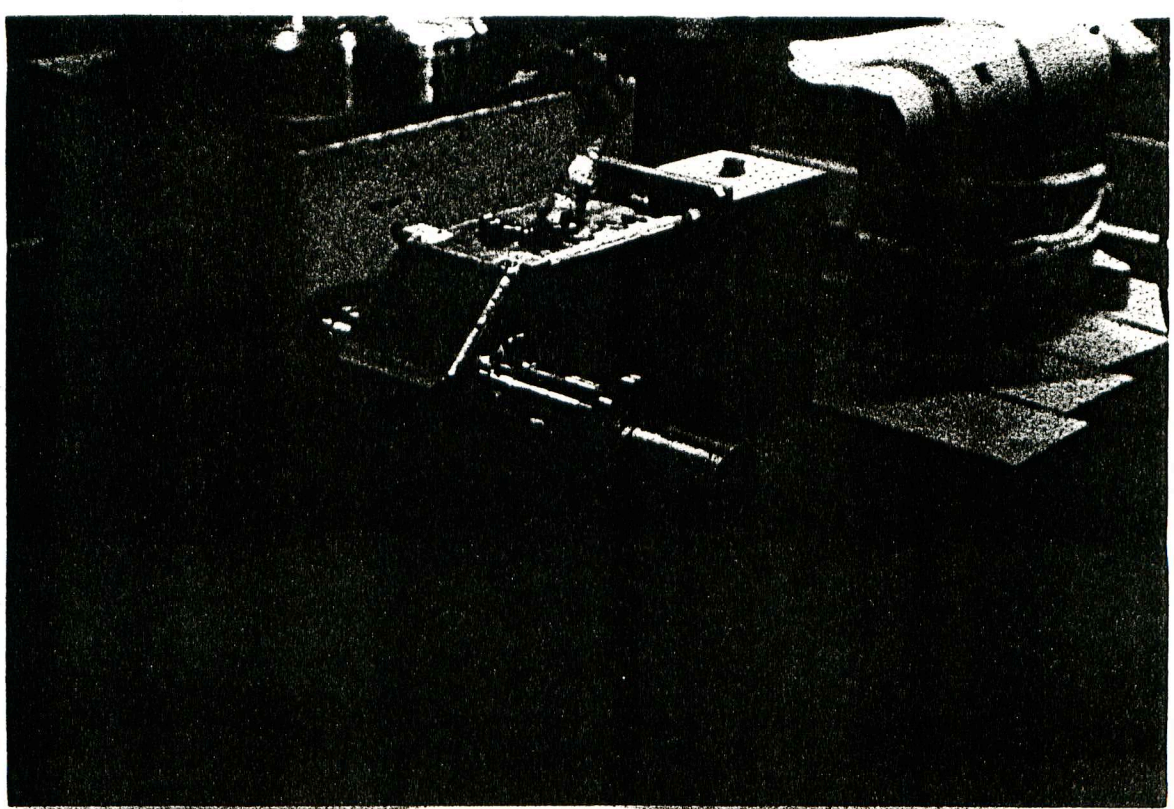

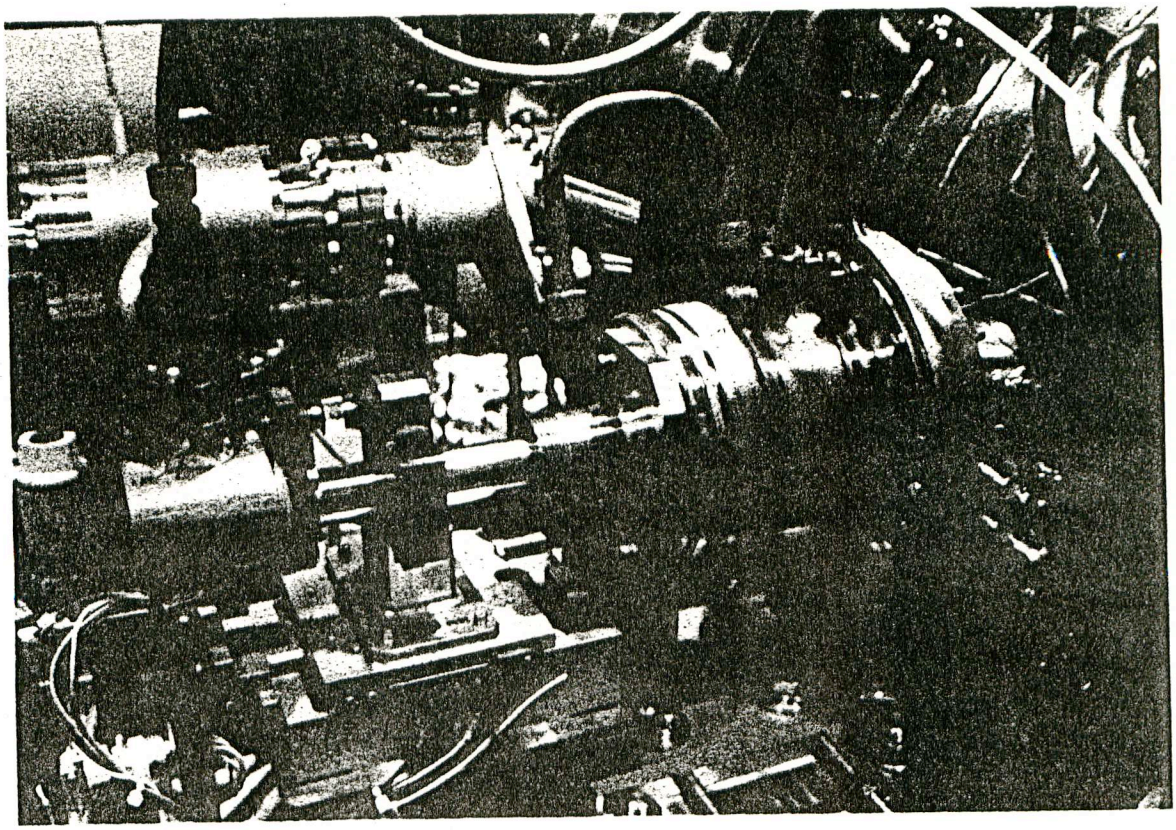

Tuner (TRISTAN APS Cavity)

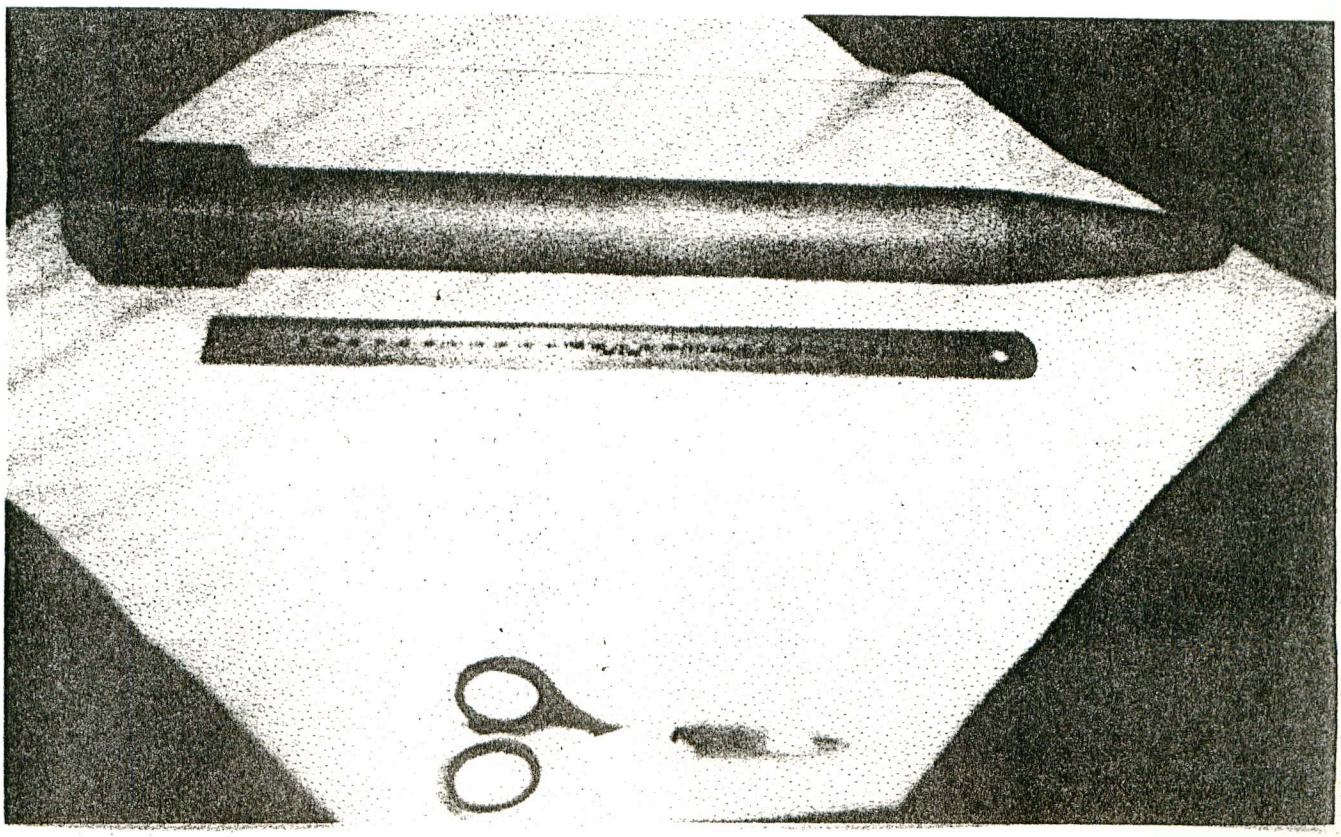

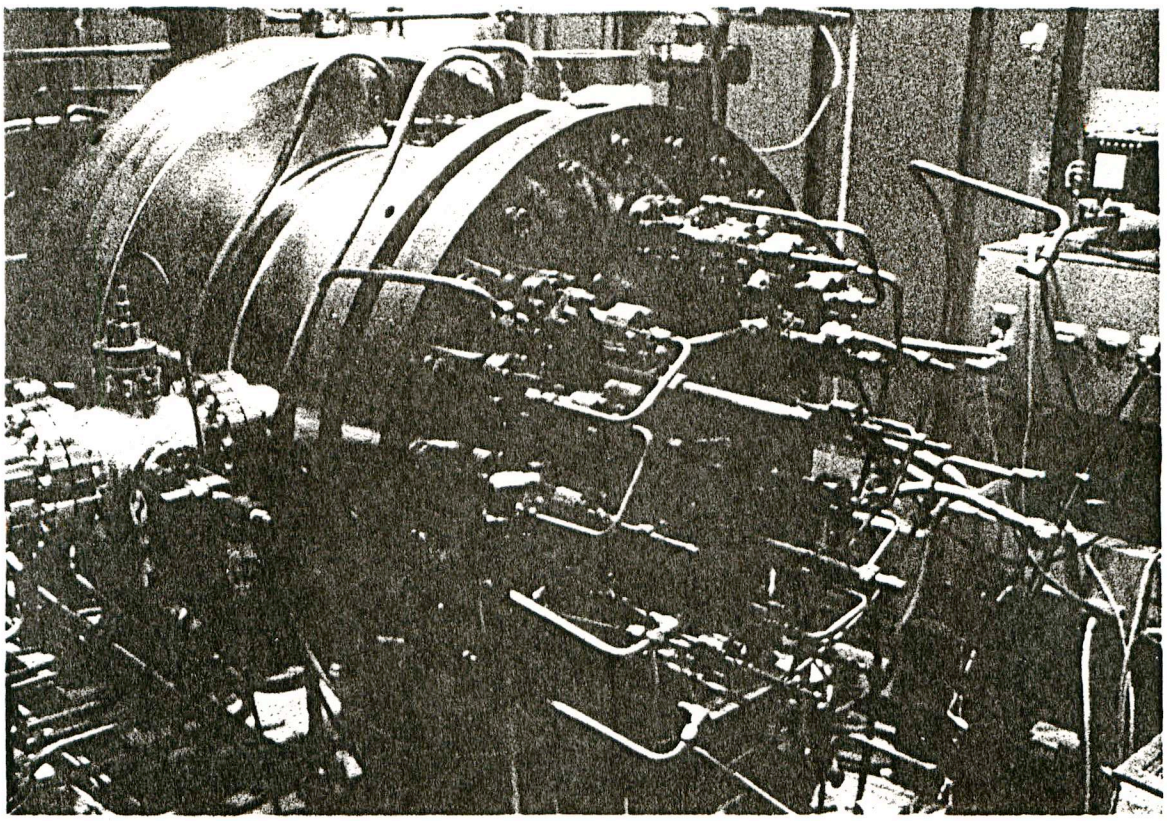

Cooling Water Circuits for SiC Absorbers